Geomorphology 427 (2023) 108619

Contents lists available at ScienceDirect

Geomorphology

journal homepage: www.journals.elsevier.com/geomorphology

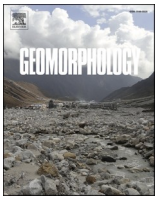

Characteristics and formation of bedrock mega-grooves (BMGs) in glaciated terrain: 1 - morphometric analyses

Mihaela Newton, Chris R. Stokes, David H. Roberts, David J.A. Evans *

Department of Geography, Durham University, South Road, Durham DH1 3LE, UK

ARTICLE INFO

Keywords:
Bedrock mega-groove
Morphometry
Glacial erosion
Abrasion
Plucking
Geological control

ABSTRACT

Bedrock mega-grooves (BMGs) are subglacial landforms of erosion that occur in glaciated terrain in various geological and (palaeo)glaciological settings. Despite a significant literature on BMGs, no systematic morphometric analysis of these landforms has been undertaken. This is a necessary step towards exploring BMG formation and has been successfully applied to other subglacial landforms of similar magnitude (e.g. mega-scale glacial lineations (MSGLs) and drumlins). In this study, BMGs from ten locations across the world are systematically mapped, sampled and measured. Based on the 10th–90th percentile of the aggregated global population (n = 1242), BMGs have lengths of 224–2269 m, widths of 21–210 m, depths of 5–15 m, elongation ratios of 5:1–41:1, and the spacing between adjacent grooves is 35–315 m. Frequency distributions for all metrics are unimodal, strongly suggesting that the sampled BMGs form a single landform population. This establishes the BMG as a geomorphic entity, distinctive from other subglacial landforms. The variability of the metrics and their correlations between and within sites most likely reflect site-specific geological characteristics. At sites which have been associated with fast-ice flow, BMGs display the largest dimensions (especially in terms of length, depth and width) but lowest elongation ratios, whereas BMGs formed under a primary geological control occupy smaller size ranges and have higher elongation ratios. Morphometrically, BMGs and MSGLs plot as different populations, with BMGs being on average 4 × shorter, 3.5 × narrower, 3.5 × more closely spaced and about 2 × deeper. It is suggested that future research focuses on numerical modelling experiments to test rates of erosion in different bedrock lithologies under varying glaciological conditions, and on adding to the body of existing field-derived empirical observations. The latter remains key to validating geological controls over BMG formation and assessing the efficiency of erosion mechanisms.

1. Introduction

BMGs are assemblages of straight grooves eroded in bedrock, typically several hundred meters long, which occur within the limits of Late Quaternary ice sheets, often juxtaposed with other subglacial landforms and aligned parallel with palaeo-ice flow directions (Smith, 1948; Gravenor and Meneley, 1958; Funder, 1978; Witkind, 1978; Heikkinen and Tikkanen, 1989; Bradwell, 2005; Bradwell et al., 2008; Eyles, 2012; Lowe and Anderson, 2003; Krabbendam et al., 2016; Newton et al., 2018). Based on these observations, BMGs have been unanimously interpreted as having formed subglacially, primarily through glacial erosion in bedrock (Smith, 1948; Gravenor and Meneley, 1958; Funder, 1978; Witkind, 1978; Heikkinen and Tikkanen, 1989; Bradwell, 2005; Bradwell et al., 2008; Jezek et al., 2011; Eyles, 2012; Krabbendam et al., 2016; Newton et al., 2018). The subglacial origin of BMGs has raised awareness of their potential for unravelling geomorphic processes at the ice–bedrock interface, as well as possible links to (palaeo) ice flow conditions, especially ice-streaming (Bradwell et al., 2008; Eyles, 2012; Krabbendam et al., 2016; Eyles et al., 2018).

Two questions are at the core of BMG research (Newton et al., 2018): i) how did BMGs form; and ii) what are the implications of BMGs for palaeoglaciological reconstructions? Regarding the first question, many authors have explored scenarios of groove formation in relation to either erosion directly by glacier ice (Smith, 1948; Gravenor and Meneley, 1958; Funder, 1978; Heikkinen and Tikkanen, 1989; Bradwell, 2005; Krabbendam and Bradwell, 2011; Eyles, 2012) or by meltwater (Sharpe and Shaw, 1989; Shaw, 2002; Bradwell, 2005). It has been noted that certain lithologies (e.g. limestone, sandstone, conglomerate, gneiss) have favoured groove formation primarily through glacial abrasion (Smith, 1948; Funder, 1978; Heikkinen and Tikkanen, 1989; Eyles,

* Corresponding author.
E-mail address: d.j.a.evans@durham.ac.uk (D.J.A. Evans).

https://doi.org/10.1016/j.geomorph.2023.108619
Received 11 November 2022; Received in revised form 3 February 2023; Accepted 4 February 2023
Available online 10 February 2023

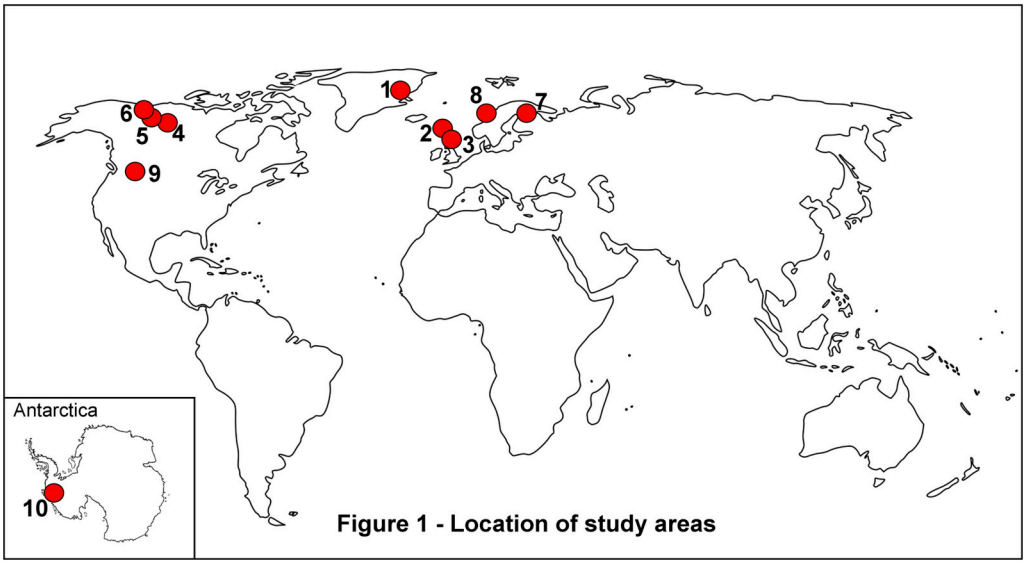

Fig. 1. Location of study areas. 1 – Haarefjord; 2 – Elphin; 3 – Ullapool; 4 – Franklin; 5 – Hanna; 6 – Beavertail; 7 – Iivaara; 8 – Vikna; 9 – Hazelton; 10 – Pine Island. The study areas are referred to by their site ID. More details about the exact location and physical characteristics of each site are presented in Table 1. The site numbering follows the order in which the sites were mapped and sampled, which is reflected throughout the structure of this paper (e.g. Fig. S1 in Supplementary Information 1).

Table 1
Summary of general information of the ten BMG sites analysed in this study, with regards to location, source of aerial imagery and bedrock lithology. For more detailed information please refer to Section 3. Abbreviations: a.s.l. = above sea level; b.s.l. = below sea level; BC = British Columbia; Mts = mountains; NT = Northwest Territories; NLSF = National Land Survey of Finland; NHS = Norwegian Hydrographic Service; Rng = range. Throughout the paper the sites are referred to by their ID name (first column).

Site ID	Location & position	Reference	Latitude/ longitude	Elevation range (m)	Area km^2	Data type/ provider	Horizontal gridding (m)	Vertical accuracy (m)	Bedrock lithology	Control	Ice streaming
Haarefjord	Scoresby Sund, Greenland, onshore	Funder (1978)	N 70°57′ W 27°56′	0–305 a.s.l.	31.2	DigiGlobe satellites – ArcticDEM	2	<1	Conglomerate	No	Not known
Elphin	West of Elphin Scotland, UK onshore	Bradwell (2005)	N 58° 3′ W 5°3′	140–295 a. s.l.	2.3	Airborne Radar (IFSAR) – NextMAP	5	1 m	Quartzite	Yes	Yes
Ullapool	Assynt, Scotland, UK onshore	Bradwell et al. (2008) Krabbendam and Bradwell (2011)	N 57°56′ W 5°2′	220–430 a. s.l.	44.9	Airborne Radar (IFSAR) – NextMAP	5	1	Meta-sandstone	Yes	Yes
Franklin	Franklin Mts, NT Canada onshore	Smith (1948)	N 65°7′ W 124°49′	130–340 a. s.l.	119	DigiGlobe satellites – ArcticDEM	2	<1 m	Limestone, sandstone, shale	No	Possible
Hanna	Hanna River, NT Canada onshore	Smith (1948)	N 65°40′ W 128°28′	150–360 a. s.l.	4.2	DigiGlobe satellites – ArcticDEM	2	<1	Sandstone	Not known	Not known
Beavertail	Beavertail Range NT Canada onshore		N 65°52′ W 128°48′	130–260 a. s.l.	2.7	DigiGlobe satellites – ArcticDEM	2	<1	Sandstone	Not known	Not known
Iivaara	Kuusamo, Eastern Finland onshore	Sutinen et al. (2010)	N 65°47′ E 29°41′	320–450 a. s.l.	2	Laser scanning – NLSF	2	<0.5	Syenite	No	Yes
Vikna	Trøndelag Platform, West Norway offshore	Ottesen et al. (2002, 2005)	N 64°57′ E 10°23′	180–235 b. s.l.	43	Multibeam swath bathymetry – NHS	50	4–6	Likely sedimentary	No	Yes
Hazelton	West of New Hazelton, BC Canada onshore	Krabbendam et al. (2016)	N 55°16′ W 127°50′	1300–1530 a.s.l.	2	Satellite – Google Earth Pro	–	–	Sandstone	No	Yes

2012; Eyles et al., 2016), whereas the BMGs present in densely jointed meta-sedimentary bedrock owe their formation mainly to glacial plucking (Zumberge, 1955; Krabbendam and Bradwell, 2011). These observations remain mostly qualitative and site-specific whereas a quantitative approach based on landform metrics would enable groove analysis at a larger scale and across sites of different lithologies. This has the potential to reveal common features leading to more generalised conclusions and overarching hypotheses on BMG genesis.

Regarding the second question, several recent studies advocate that BMGs form in onset zones of fast-flowing ice (palaeo-ice streams) through focussed bedrock erosion, enhanced by high ice-flow velocities and in conjunction with meltwater erosion (Lowe and Anderson, 2003; Bradwell et al., 2008; Eyles, 2012; Smith et al., 2012; Krabbendam et al., 2016; Eyles et al., 2018). This is based on BMGs within palaeo-ice stream landsystems, being associated with other elongate subglacial bedforms such as MSGLs and rock drumlins (Bradwell et al., 2008; Lowe and Anderson, 2003; Eyles, 2012; Krabbendam et al., 2016). However, doubt has been expressed regarding fast-ice flow as a precondition for BMG formation (Newton et al., 2018), given that BMGs also occur in areas not affected by ice streaming (e.g. Funder, 1978) or where the evidence for ice streaming is equivocal (e.g. Brown, 2012). Additionally, some BMGs appear to owe their development to long-term glacial erosion controlled by the bedrock geology, despite being situated within palaeo-ice stream landsystems (e.g. Roberts et al., 2010; Newton, 2022). Morphometric comparisons between BMGs and other large-scale subglacial landforms of similar shape, namely MSGLs, may help to clarify to what extent BMGs and MSGLs share morphogenetic similarities and elucidate the role of fast-ice flow in BMG formation.

Elsewhere in glacial geomorphology, quantitative analyses of landform metrics have led to important advances in the understanding of streamlined subglacial landforms such as ribbed moraine (Dunlop and Clark, 2006), drumlins (Clark et al., 2009; Ely et al., 2018), MSGLs (Stokes et al., 2013; Spagnolo et al., 2014), eskers (Storrar et al., 2014) and flutings (Ely et al., 2016). Specifically, the availability of morphometric data derived from systematic measurements of large landform populations has enabled statistical analysis of pattern distributions, as well as comparisons within and between groups of landform populations (Hillier et al., 2013; Hillier et al., 2016). The results have been used to test formation hypotheses (Stokes et al., 2013; Spagnolo et al., 2014), endorsed the previously proposed connections with ice streaming (Clark, 1993) and enabled a deeper exploration into landform continua (Stokes et al., 2013; Ely et al., 2016). Large samples of empirical data on subglacial landform metrics have also been used to test numerical models of landform formation (e.g. Dunlop et al., 2008; Livingstone et al., 2015).

Despite BMGs generally being recognised as a distinctive landform category in the wider range of subglacial bedforms, their dimensions have never been quantitatively established using systematic mapping and sampling from a sample of global data. Studies spanning over 100 years of research report mean values for landform metrics extracted from various sites and following different protocols, which cannot form a suitable basis for global quantitative analysis due to inherent inconsistencies. Few site-specific studies have undertaken measurements systematically (e.g. Gravenor and Meneley, 1958; Bradwell et al., 2008) or on large enough population samples for the results to be statistically robust. Additionally, older BMG studies have provided only general information on landform dimensions (e.g. Smith, 1948; Funder, 1978).

In this paper we provide the first quantification of the size, shape and spacing of bedrock mega-grooves (BMGs) across a range of settings (Fig. 1), in order to better understand the characteristics and origin of these enigmatic landforms. Consistent measurement protocols have been applied systematically to produce sufficient data for robust quantitative analyses (Chandler et al., 2018). Specifically, we aim here to: i) constrain the dimensions of BMGs; ii) highlight and explain landform distribution patterns, particularly in relation to bedrock lithology; iii) compare BMGs to MSGLs and use the results to further explore links with ice streaming; and iv) gain deeper insight into possible overarching conditions for BMG formation based on correlations between metrics. The resulting database of BMG metrics is of comparable complexity and magnitude to that existing for MSGLs (Spagnolo et al., 2014) and is used to further analyse the morphometry and distribution of BMGs. The problem of BMG initiation remains to be addressed comprehensively based on a suitable empirical database and so, following on from this paper, Evans et al. (2023 – Part 2) have used the data presented here to compile and propose some theoretical and conceptual models of BMG initiation for further hypothesis testing.

2. Methods

2.1. Digital datasets

DEMs at various resolutions were used for landform mapping and measurement at all sites except Hazelton, for which 2D Google Earth imagery was used instead (Table 1). NEXTMap digital terrain model (DTM) files were used for the two Scottish sites, at Elphin and Ullapool, available through https://www.intermap.com/nextmap. The NEXTMap DTM is a bare-earth model containing elevations of natural terrain features in the UK, whereby elevations of vegetation and anthropogenic artefacts have been digitally removed. The resolution is 5-m posting and it has a vertical accuracy of 1 m root-mean-square error in unobstructed areas with slopes $<10^{\circ}$. The data rendition on DTMs is void-free and seamless, as the data-collecting technology is not hindered by any weather effect or cloud coverage.

The ArcticDEM files used for Haarefjord, Franklin, Hanna and Beavertail are stereo-derived elevation models covering high-latitude terrain and are downloadable directly from https://www.pgc.umn.edu/data/arcticdem/. The in-track and/or cross-track stereo imagery was collected by satellites and processed into 2-m posting using photogrammetric techniques. The files used in this study are mosaic files obtained by joining multiple strips, which have been co-registered, blended and feathered to reduce the edge-matching effects. One weakness is that the terrain image is not a bare-earth product because the vegetation and any human interference and infrastructure add to the overall ground elevation, whereas water surfaces (e.g. lakes) obscure any submerged topography. As the product is optically derived, there are sometimes data voids resulting from atmospheric obstruction present at the time of data acquisition (e.g. clouds, fog, shadows). Overall, the accuracy is approximately 2 m in horizontal and vertical planes.

The elevation model for the site at Vikna, located on the Norwegian continental shelf, was obtained through the Norwegian Hydrographic Service https://kartkatalog.geonorge.no/. The hydrographic survey data were compiled in the form of a 50-m resolution DEM from depth measurements using multibeam echo sounders, laser and single beam echo sounders.

The DEM for the Iivaara site, provided by the National Land Survey of Finland through https://www.maanmittauslaitos.fi/en/maps-and-spatial-data, has a grid size of 2 × 2 m and is based on laser scanning data with a point density of at least 0.5 points per m^2. The accuracy of the elevation data is 0.3–1 m.

The topographic data for the continental shelf at Pine Island Bay, Antarctica were collected through multibeam swath bathymetry at a scale of tens of meters and processed into a hill-shaded terrain model, with features smaller than 10 m recorded locally using a deep-tow apparatus (Lowe and Anderson, 2002). The data were collected between 1999 and 2010 and later compiled into a comprehensive 35-m grid by Nitsche et al. (2013), available to view and manipulate in 3D in GeoMapApp http://www.geomapapp.org/.

The raw DEMs were imported and rendered in ArcMap, following best practice outlined in Smith and Clark (2005) for optimum visualisation of linear landforms. Thus, the DEMs used as a mapping base were rendered as greyscale hill-shaded terrain and the light-source azimuth was applied perpendicular to the mega-grooves at an illumination height of 45°. The DEMs were also viewed with the light source parallel to the mega-grooves/ridges, which made the landforms less obvious, but still observable, due to their large dimensions. This was done to rule out illumination biases known to produce false appearance of landforms. The imagery from Pine Island Bay, Antarctica was visualised in GeoMapApp where the 3D-effect is obtained through altitude colour-coding.

Table 2
Summary statistics for BMG metrics. The mode was established based on a visual examination of the graphs, whereby those graphs with a clear peak were regarded as unimodal.

Metric	Summary statistics	Haarefjord	Elphin	Ullapool	Franklin	Hanna	Beavertail	Iivaara	Vikna	Hazelton	Pine Isl.	All sites
Length	No. of BMGs	162	37	248	397	64	37	87	74	37	99	**1242**
	Min	65	94	135	113	167	155	57	302	136	450	**57**
	10 pct	142	177	356	243	356	361	113	533	223	908	**224**
	Median	447	382	843	661	656	605	316	1117	445	1580	**662**
	Mean	594	449	1039	1228	776	610	352	1350	439	1888	**1018**
	90 pct	1203	688	2032	2760	1303	877	628	2487	671	3330	**2269**
	Max	2628	1465	4258	9713	1867	1259	1354	3200	854	4210	**9713**
	Std dev	508	272	734	1357	417	241	242	752	176	956	**1005**
	Mode	200–300	200–300	400–500	300–500	600–600	Polymodal	100–200	800–900	400–500	1500–1600	**400–500**
Width	No. of BMGs	18	12	33	40	38	30	30	20	34	21	**276**
	No. of data points	259	61	416	640	359	211	202	213	170	255	**2966**
	Min	11	24	30	28	22	30	7	105	8	20	**7**
	10 pct	19	36	60	55	34	40	13	145	13	100	**21**
	Median	30	71	88	130	55	60	22	218	18	180	**76**
	Mean	30	74	91	137	58	64	23	220	18	180	**98**
	90 pct	43	110	130	223	85	95	35	280	23	260	**210**
	Max	55	160	194	370	114	150	56	450	43	500	**370**
	Std dev	9	29	28	65	19	22	9	61	5	61	**75**
	Mode	20–30	60–70	70–90	Polymodal	50–60	50–70	10–30	Polymodal	10–20	200–210	**20–30**
Lateral spacing	No. of BMG pairs	25	26	36	57	49	33	47	26	32	24	**355**
	No. of data points	207	124	447	757	332	197	210	233	143	363	**2986**
	Min	19	35	38	37	19	6	10	121	10	127	**6**
	10 pct	27	43	58	74	39	54	19	207	17	159	**35**
	Median	42	80	88	142	68	87	30	300	30	270	**95**
	Mean	45	86	82	158	72	100	35	313	37	271	**134**
	90 pct	62	126	112	289	116	158	59	404	77	362	**315**
	Max	109	246	145	405	172	262	110	734	126	421	**405**
	Std dev	16	42	20	79	29	48	19	104	22	72	**104**
	Mode	40	72	84	142	73	112	30	295	27	149	**84**
Depth	No. of BMGs	18	14	33	40	38	30	30	20	–	21	**244**
	No. of data points	259	72	416	640	359	211	202	213	–	255	**2627**
	Min	1	1	1	1	1	1	1	1	–	1	**1**
	10 pct	2	2	2	1	2	2	1	3	–	5	**2**
	Median	4	7	6	3	5	5	2	7	–	14	**5**
	Mean	4	7	7	5	6	6	2	8	–	18	**7**
	90 pct	7	14	13	13	13	10	3	15	–	40	**15**
	Max	13	20	25	63	20	27	6	40	–	60	**63**
	Std dev	2	5	4	6	4	4	1	6	–	13	**7**
	Mode	4	5	5	5	3	3	1	6	–	10	**3**
Elongation	No. of BMGs	18	12	33	40	38	30	30	20	34	21	**276**
	No. of data points	N/A	N/A	N/A	N/A	N/A	N/A	N/A	N/A	N/A	N/A	**N/A**
	Min	20	4	9	3	6	4	9	2	11	4	**2**
	10 pct	23	5	10	6	9	5	11	3	12	5	**5**
	Median	41	8	21	22	15	9	22	5	25	7	**15**
	Mean	42	10	22	25	16	10	27	5	25	7	**20**
	90 pct	63	15	32	45	24	15	46	8	38	11	**41**
	Max	72	19	49	99	42	18	59	10	50	14	**99**
	St dev	16	4	10	19	7	4	15	2	11	3	**15**
	Mode	Polymodal	Polymodal	Polymodal	Polymodal	Polymodal	Polymodal	Polymodal	4–6	Polymodal	4–6	**8–10**
Azimuth	No. of BMGs	199	36	371	757	109	41	87	83	–	–	**–**
	Min	71	258	246	157	272	298	111	271	–	–	**–**
	10 pct	116	272	264	240	280	306	119	297	–	–	**–**
	Median	119	284	274	265	290	311	124	302	–	–	**–**
	Mean	119	281	274	262	286	311	124	302	–	–	**–**
	90 pct	123	288	285	276	299	314	128	308	–	–	**–**
	Max	143	292	299	280	304	329	136	323	–	–	**–**
	Std dev	5	8	8	14	22	5	4	7	–	–	**–**
	Mode	119	285	270	266	297	313	124	303	–	–	**–**
BMG density	No. of BMGs/area (grooves/km^2)	31.2	14.8	5.7	3.1	15.2	13.5	43.5	1.7	12.3	0.7	
	BMG length/area (km^{-1})	18.6	17.5	5.8	3.8	11.8	8.21	15.33	2.3	8.1	1.3	

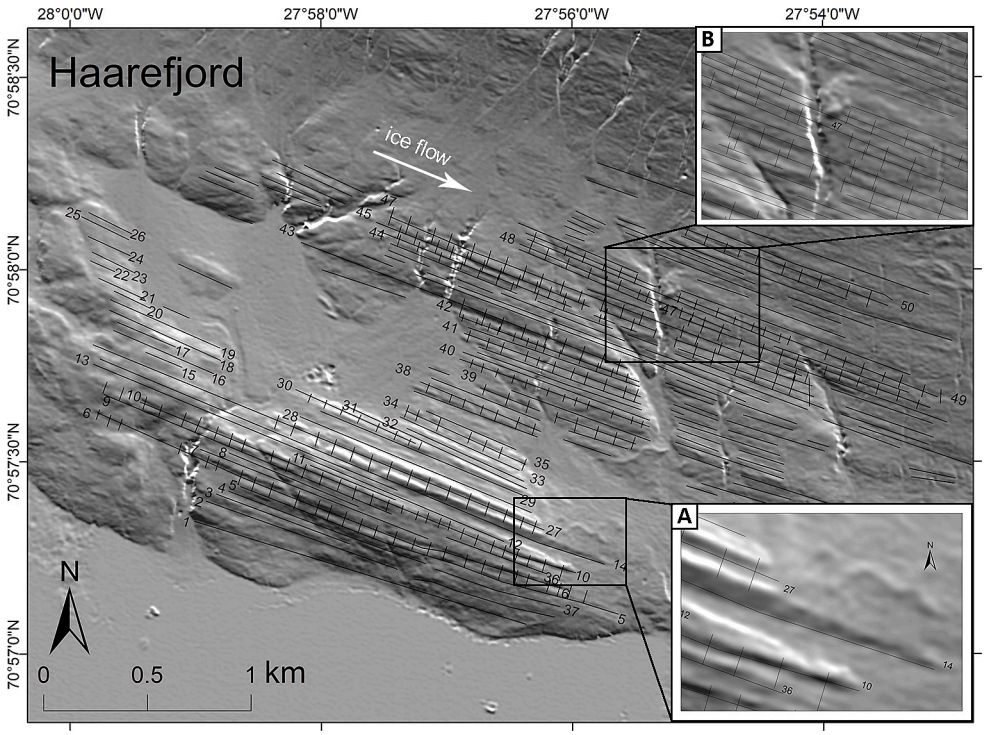

Fig. 2. Example of a sampled site (Haarefjord), showing the location of the cross-profiles on which depth and width were measured. The numbered BMGs with cross-profile transects represent those BMGs for which depth and width were measured. The numbered BMGs with no cross profile transects (e.g. 15–26) were used for measuring lateral spacing. For the remaining nine sites the sampled grooves and the data point locations are represented in Fig. S1 in Supplementary Information 1: A) BMG mapping in relation to the bounding ridges, whereby the groove end-point corresponds to the shortest of the two ridges (e.g. groove 27); B) BMG mapping in areas of cross-cutting channels, where BMGs are mapped as continuous lines only where groove continuity can be visually matched on both sides of the cross-cutting landform. Base images Arctic DEM.

2.2. BMG mapping and sampling

BMGs were identified on the DEMs as multiple straight and parallel features aligned in the ice flow direction, visually enhanced by the differences in shading where the angle of slope exposure to the light source changes. As the same visual effect occurs along ridges, cross profiles were traced where in doubt, to ensure that the focus remained on the grooves. Cross-profiles were traced to verify the BMG presence in the topography where the shading variation was hardly visible due to groove shallowness. In cases where the bounding ridges were of different length, establishing the start/end point of a BMG was guided by the shortest of the two ridges, despite the change in shading being visible along the longer ridge. BMGs were mapped as continuous lines over cross-cutting bedrock incisions only where their continuation was visually unequivocal on aerial imagery. At Ullapool and Haarefjord this may have influenced the result for groove length as well as the overall number of landforms (see Section 5.1). Following these assessments, the BMGs were mapped as solid lines along the deepest part of the groove. A total of 1242 BMGs were mapped across all sites (Table 2).

In order to select the areas best suited for sampling and minimise interference from other landforms or geological features, geomorphic mapping was more detailed. Thus, linear features other than BMGs were also mapped, for example breaks of slope along geological fractures, and faults aligned across the grooved area or along lithological contacts, or changes in the general aspect of topography. Areas of fluvial erosion or deposition interspersed with, or superimposed on, the grooved terrain were also mapped, as well as areas of glacifluvial deposits or infilled basins. Where possible, maps were checked against pre-existing geomorphic and geological maps. BMG sampling was avoided in areas where other landforms and deposits were widely present, as these could potentially have altered groove profiles and resulted in unrealistic values for groove metrics (see Section 2.4).

At each site, BMGs were sampled for length, width, depth and lateral spacing. At Hazelton, where only 2D measurements could be carried out, no data for groove depth was obtained. There were large variations in the number of grooves across sites (e.g. 37 at Elphin, Beavertail and Hazelton compared to 397 at Franklin). Consequently, at sites comprising fewer than 40 grooves, we aimed to sample entire groove populations, leaving out the grooves with a poorly defined cross-profile (Fig. S1 in Supplementary Information 1), while at sites with a large number of landforms, approximately 15 % of grooves were sampled to balance the time incurred with the aim of obtaining representative data (c.f. Spagnolo et al., 2014). The exact number of features sampled for each metric, as well as the number of data points at each individual site, are recorded in Table 2.

2.3. BMG measurements

The length, depth, width and lateral spacing of the BMGs were measured using semi-automated methods facilitated by tools and features in ArcMap, GeoMapApp and Google Earth. Length was automatically retrieved in ArcMap from the attribute table of shape files, whereby each polyline corresponds to an individual groove. At Hazelton and Pine Island, BMGs were manually measured in Google Earth and GeoMapApp, respectively. Width, depth and lateral spacing were measured in the palaeo-ice flow direction at 100-m intervals (Fig. 2; Fig. S1 in Supplementary Information 1). To correctly gauge the distance between data points, a fishnet overlay was applied on the DEM in ArcMap, or a digitised graded-ruler guide was moved along each groove and metrics were extracted manually. The minimum number of data points for each sampled groove was three. The sampling protocols were followed as closely as possible, but sometimes small compromises had to be made to keep the measurements systematic. Thus, occasionally the cross-profile location had to be shifted up to a few 10s of metres along the groove in order to avoid interference with cross-cutting geological features (e.g. fault lines, fractures) or erosional/depositional features (e.g. meltwater channels/eskers).

Measurement of depth and width first required the identification of the groove as a geomorphic entity. This equates to establishing the groove's upper and lower limit, or separating groove from ridge, to ensure the measurements remained focused on the groove. As grooves and ridges exist in conjunction with each other, it can be difficult to clearly distinguish between them when the top of the groove does not coincide with the crest of the intervening ridge. The protocol followed

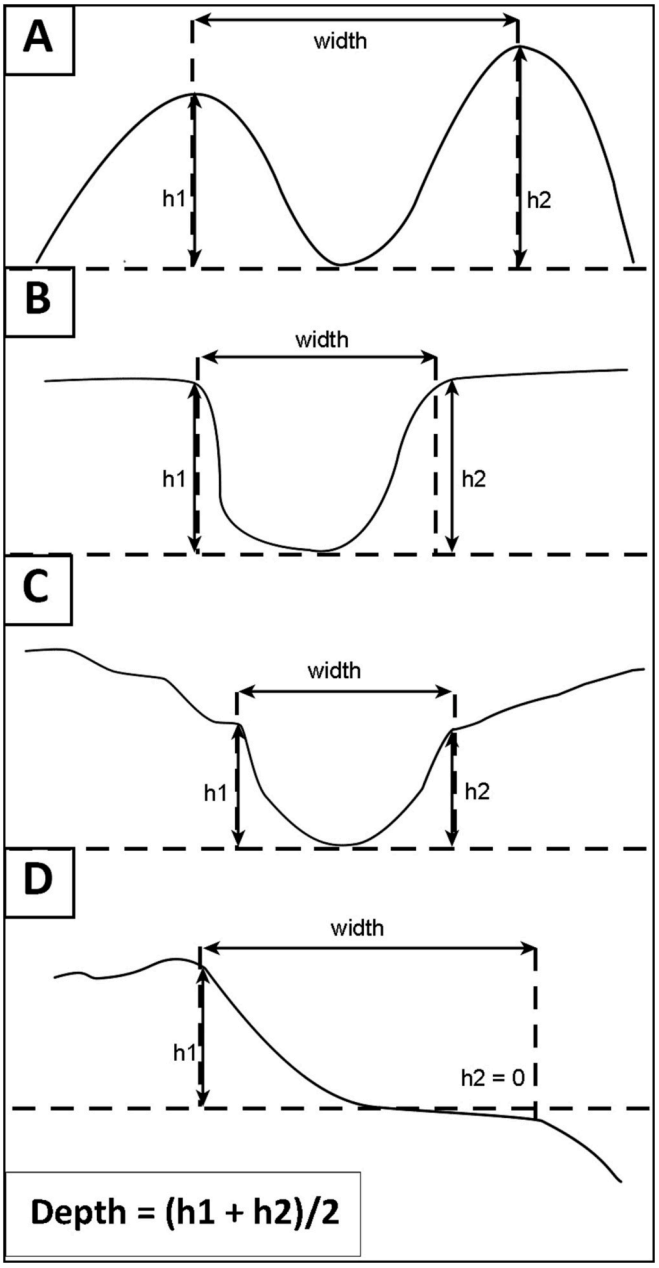

Fig. 3. Measurements of groove width and depth on different types of BMG cross-profile: A) sinusoidal profile where the grooves mirror the ridges; B) grooves eroded into a relatively flat surface; C) grooves defined by convex inflections in the cross profile, situated at similar altitude on opposite flanks; D) grooves with a stepped profile, with only the flank defined in the topography.

here is summarised in Fig. 3, whereby the top of the groove represents the point of maximum inflexion on the flank profile (c.f. Spagnolo et al., 2014). It was found that most cross profiles fell into one of four categories. In the case of sinusoidal profiles, the peak of the ridge is also the uppermost part of the groove (Fig. 3A). Where the grooves were eroded into a relatively flat, plateau-like surface, the top of the groove coincides with the plateau edge (Fig. 3B). Where the cross-profile had an irregular shape, the break of slope closest to the groove floor was considered to be the top of the groove flank. In cross-profile this occurs either as a ledge eroded into the slope of the ridge or a change in the slope convexity (Fig. 3C). Often there is an inflexion in the slope profile on the opposite ridge, at a matching altitude, except for grooves with a stepped profile, where typically only one side is well defined (Fig. 3D). Once the groove geometry was established, depth was calculated as the average height of

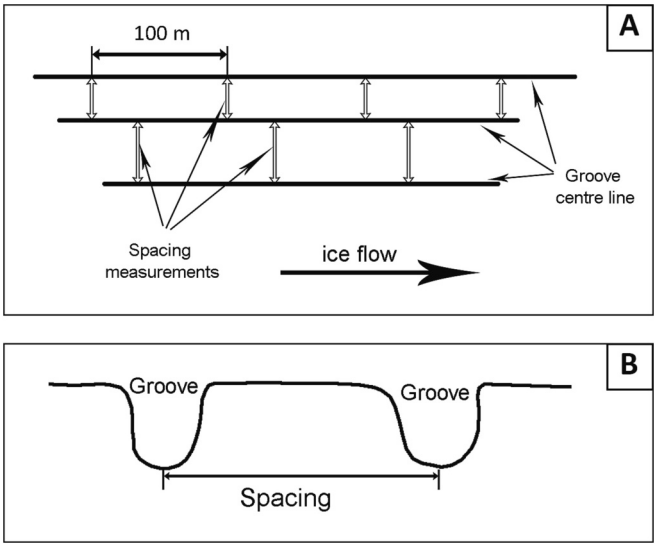

Fig. 4. Schematic representation of spacing measurements: A) along adjacent grooves at 100-m intervals in the ice-flow direction; B) between the centre line of adjacent grooves. Ice flow direction perpendicular to the page.

the two flanks, and width was measured as the distance between the uppermost limit of the two groove flanks (Fig. 3). Spacing was measured at 100-m intervals along the ice-flow direction (Fig. 4A) as the distance between the centre-line (i.e. groove floor) of two adjacent grooves (Fig. 4B).

For azimuth calculations, the grooves mapped as polylines were first split at vertices, which resulted in a series of segments, so that the azimuth could be calculated for each segment using ArcGIS tools. The summary statistics were subsequently calculated based on the azimuth values for individual segments between vertices rather than the individual grooves. However, the majority of the BMGs were mapped as straight lines rather than polylines. The elongation ratios (length:width) were calculated only for the grooves with measured widths, by dividing the mean length value by groove width.

2.4. Errors and uncertainties

Most sites were mapped and sampled on high-resolution imagery (see Section 2.1), with horizontal gridding of 2–5 m and vertical accuracy of at least 1 m (Table 1), thereby making BMGs fully visible. Any grooves narrower than 2–5 m or shallower than 1 m, which may not have been identified, are not mega-grooves per se and are better described as a macro- or meso-grooves (Newton et al., 2018). At Pine Island and Vikna, where the horizontal resolutions of the DEMs were 35 m and 50 m, respectively, some BMGs may have not been visible and therefore were not mapped, which may have resulted in higher values for lateral spacing and width. Conversely, at Iivaara, the high vertical accuracy of <0.5 m (Table 1 and Section 2.1) meant that very shallow grooves became visible and hence may have skewed the value range towards the lower end at this site. At Hazelton, the width measurements are estimations rather than exact measurements, extracted from high-quality Google Earth imagery, aided by the presence of snow inside the grooves. These represent estimated minimum values, which may have resulted in underestimations of width. These factors have been considered in the interpretation of results, where relevant.

The internal consistency of the results is ensured by the fact that the mapping and measurements at all sites were undertaken by the same person over a relatively short period of time, spanning less than 10 months, and following consistent protocols. At Haarefjord, Ullapool and Elphin, the metrics were found to be generally consistent to those reported by Funder (1978), Bradwell et al. (2008) and Bradwell (2005),

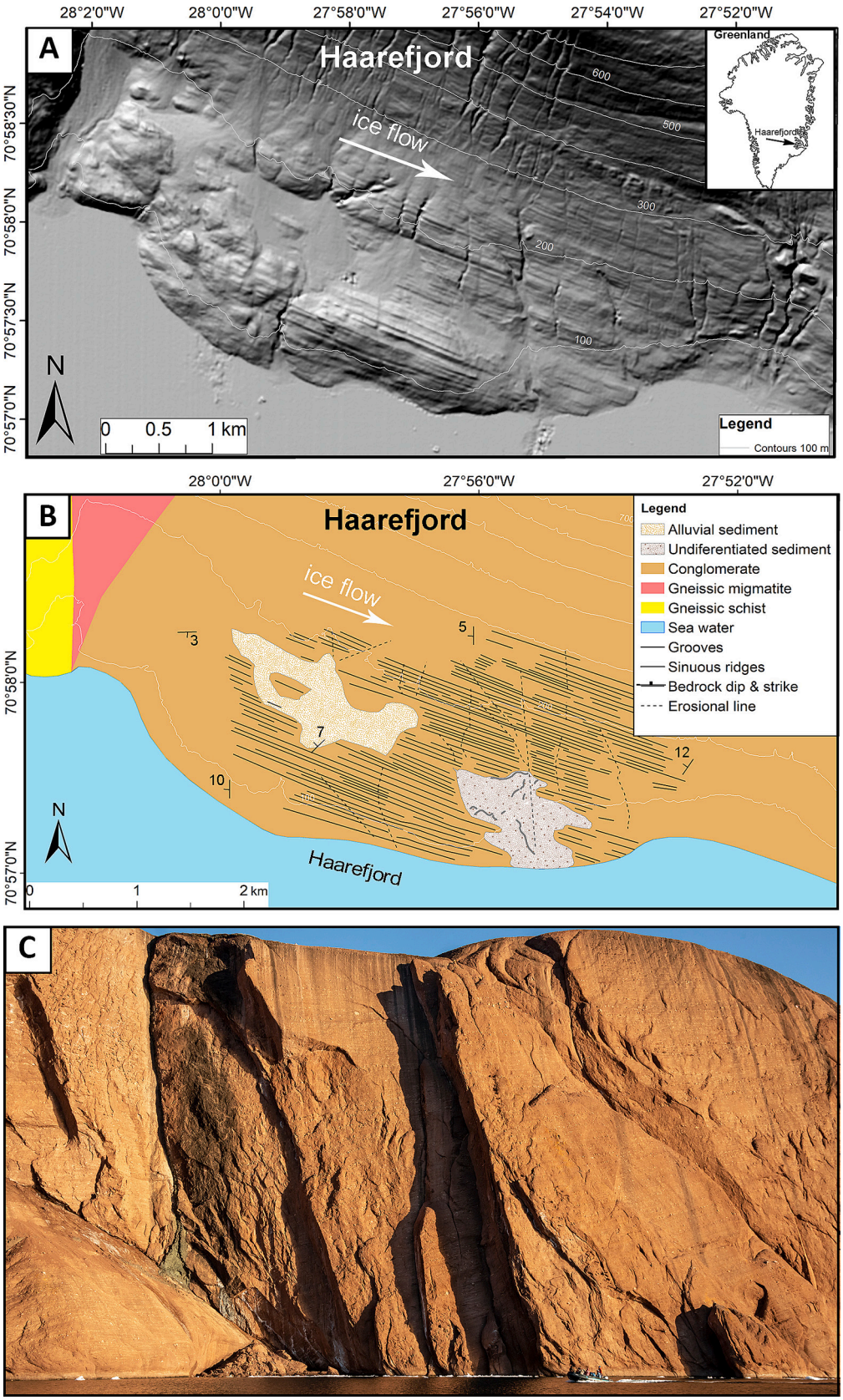

Fig. 5. The Haarefjord study site: A) Digital elevation model (Arctic DEM) of the grooved terrain at Haarefjord, inner Scoresby Sund, East Greenland. Illumination angle from the north. Inset shows location of study area in eastern Greenland. Outline of inset map © PatternUniverse.com; B) Schematic map of bedrock and surficial geology compiled from Henriksen (1983) and the Geological Map of Greenland 1: 500,000 (2014). C: Outcrop of Røde Ø conglomerate at Haarefjord. Note the massive appearance of the rock and the lack of jointed beds. Photo courtesy Terry Allen © allenfotowild.com.

respectively (Table T1 in Supplementary Information 1; see also Section 5.1). BMG mapping in areas with cross-cutting channels may have resulted in underestimation of BMG mean length by a few hundred meters. These situations are not common and only applicable to two sites out of ten, namely Ullapool and Haarefjord (see Section 2.2). While they may be of local importance (Newton, 2022), they are unlikely to have significantly altered the BMG length values in the global dataset.

In summary, the aerial imagery used here allowed for consistent measurements across sites, with only three gaps in the dataset, namely one for depth and two for azimuth values (Table 2). At most sites, the BMG visibility on the aerial imagery is excellent due to the high-resolution horizontal gridding combined with high vertical accuracy, and some data at Elphin and Ullapool were checked in the field. At Vikna and Pine Island, however, the relatively coarse resolution may have resulted in some landforms being missed, which in turn may have resulted in an overestimation of groove width and spacing. Nevertheless, the consistency in data collection from digital datasets, with similar resolution ranges used for most sites, is expected to have produced an overall robust basis for quantitative analysis.

3. Study areas

BMGs are relatively scarce compared to other subglacial landforms, with only about 20–25 sites reported worldwide (Newton et al., 2018). Of these, ten sites were selected for the purposes of this study (Fig. 1) with the aim of producing a sizeable and representative dataset. The availability of suitable imagery to measure the BMGs was an important consideration and precluded the sampling of several sites. The sites were selected according to three criteria as outlined below.

First, an assessment of the substrate was carried out to ensure that the mega-grooves occur in bedrock rather than in unconsolidated glacigenic deposits. This was in order to avoid confusion between BMGs and MSGLs, especially when considering their often-similar appearance on remotely sensed imagery (Krabbendam et al., 2016). The substrate assessments for the onshore sites were based on information from maps of solid bedrock geology and superficial deposits, in conjunction with published empirical evidence where available and with some fieldwork results (Newton, 2022). At Vikna and Pine Island, which are situated offshore, the solid bedrock substrate was inferred through geophysical investigations (e.g. Lowe and Anderson, 2003). We aimed to cover a variety of lithologies to allow for tentative correlations between groove metrics and bedrock characteristics. Overall, the study areas are devoid of unconsolidated glacigenic sediment and, where present, it is patchy and thinly draped over bedrock, thus preserving the shape of the bedrock topography underneath.

Second, the local and regional glacial history of the selected sites had to be well documented to enable assessment of groove alignment with independent indicators of palaeo-ice flow direction, as well as their subglacial origin. This assessment was particularly relevant at Beavertail and Vikna, where the BMGs have not been previously described. Reconstructions of former ice-flow direction at these sites were based on the presence of other streamlined landforms, such as drumlins, crag-and-tails and MSGLs, in conjunction with BMGs, based on studies by Smith (1948) and Ottesen et al. (2002), respectively.

The third selection criterion was ease of access to remotely sensed imagery of adequate resolution for topographic measurements. In this respect, aerial imagery for onshore sites is more widely available and in open-access format. Additionally, the resolution is higher than that for offshore sites and the substrate is usually known in more detail. Therefore, eight out of the ten chosen sites are situated onshore (Fig. 1 and Table 1).

3.1. Haarefjord

The BMGs at Haarefjord occur in a lowland area sloping gently (10–15°) in a NNE–SSW direction from 350 m down to sea level (Fig. 5A). The Røde Ø conglomerate, in which the mega-grooves occur, forms an insular outcrop surrounded by Precambrian gneissic bedrock to the west (Fig. 5B) and approximately 4 km east of the grooved terrain (Sørensen, 1970; Henriksen, 1983). The Røde Ø conglomerate typically consists of middle-late Permian, coarse sandstone and conglomerate with gneiss phenoclasts (Fig. 5C; Collinson, 1972; Stemmerik and Piasecki, 2004). The conglomerate beds show varying orientations with a low-angle dip (Fig. 5B and C), possibly reflecting different cones of deposition (Funder, 1978), and are generally massive or poorly jointed (Fig. 5C). The grooves and ridges are mis-aligned with the bedrock structure, but parallel to the palaeo-ice flow direction (Fig. 5B) and have been interpreted as being the result of glacial erosion (Funder, 1978).

Superficial deposits are present within the grooved terrain. In the west, fluviatile sediments obscure the BMGs, as indicated by the presence of grooved bedrock protruding through the sediment cover (Fig. 5B). To the south-east, an area of undifferentiated sediment (Henriksen, 1983) also obscures the bedrock grooves and ridges, as indicated by the gradual disappearance of the groove/ridge profiles (Fig. 5A). The unconsolidated sediments there are likely glacifluvial, as suggested by the presence of clustered sinuous ridges and mounds, 50–350 m long and 1–8 m in amplitude, indicative of eskers (Fig. 5B). To the north, the bedrock has several incisions 350–650 m long and 3–5 m deep which cross-cut the grooves and ridges. No horizontal displacement is apparent on the digital elevation model (DEM) imagery, and many ridges match on both sides of the incisions. However, the grooves have been mapped as continuous lines only where there is a clear landform continuation across a bedrock incision (Fig. 5B; see Section 2.2).

3.2. Elphin

The Elphin grooves occur in a lowland area and trend upslope relative to the palaeo-ice flow direction (Fig. 6A). The bedrock consists of well-bedded quartzite where initial deposition was as horizontal beds of fine-grained sediment in a shallow marine environment during the Cambrian. The beds were subsequently tilted by 12–19° to the south-east and metamorphosed into quartzite (Peach et al., 1907; Fig. 6B). The mega-grooves are eroded into a pre-existing surface, as suggested by the matching height of the intervening ridges (Fig. 6C) and are aligned slightly obliquely to the bedrock strike (Bradwell, 2005; Fig. 6A).

There is widespread evidence of glacial abrasion in the form of polished rock surfaces with shallow striations <2 mm deep and well-rounded edges to individual strata outcrops, as well as vestiges of meltwater erosion (Fig. 7A) and chattermarks (see also Bradwell, 2005). However, by far the largest volume of bedrock removed subglacially was through plucking, considering the relatively large size of plucked rocks and the abundant evidence of quarried faces across the grooved area (Fig. 7B). Block dislocation though plucking was enabled by the bedrock joint system; one near-horizontal and defined by the bedding planes, and two nearly-vertical joint systems striking sub-perpendicular to each other (see also Krabbendam and Bradwell, 2011). The plucked blocks measure on average 10 × 15 × 30 cm. The Elphin site represents an example of where glacial erosion, specifically plucking, was controlled by the geological structure, despite the groove landforms being aligned obliquely to the bedrock strike or to any other major structure.

Glaciologically, the grooved terrain at Elphin has been hypothesised to be an area of fast-flow onset along the flow corridor of a tributary glacier to the Minch Ice Stream. The latter was a topographically-constrained, marine-terminating ice stream draining the north-western sector of last British-Irish Ice Sheet, originating in the Assynt region of western Scotland and reaching the continental shelf edge (Bradwell et al., 2007, 2019). The Minch Ice Stream was initially recognised based upon its distinctive signature in the geomorphic and stratigraphic record offshore (Stoker and Holmes, 1991; Stoker, 1995; Stoker and Bradwell, 2005; Bradwell et al., 2019).

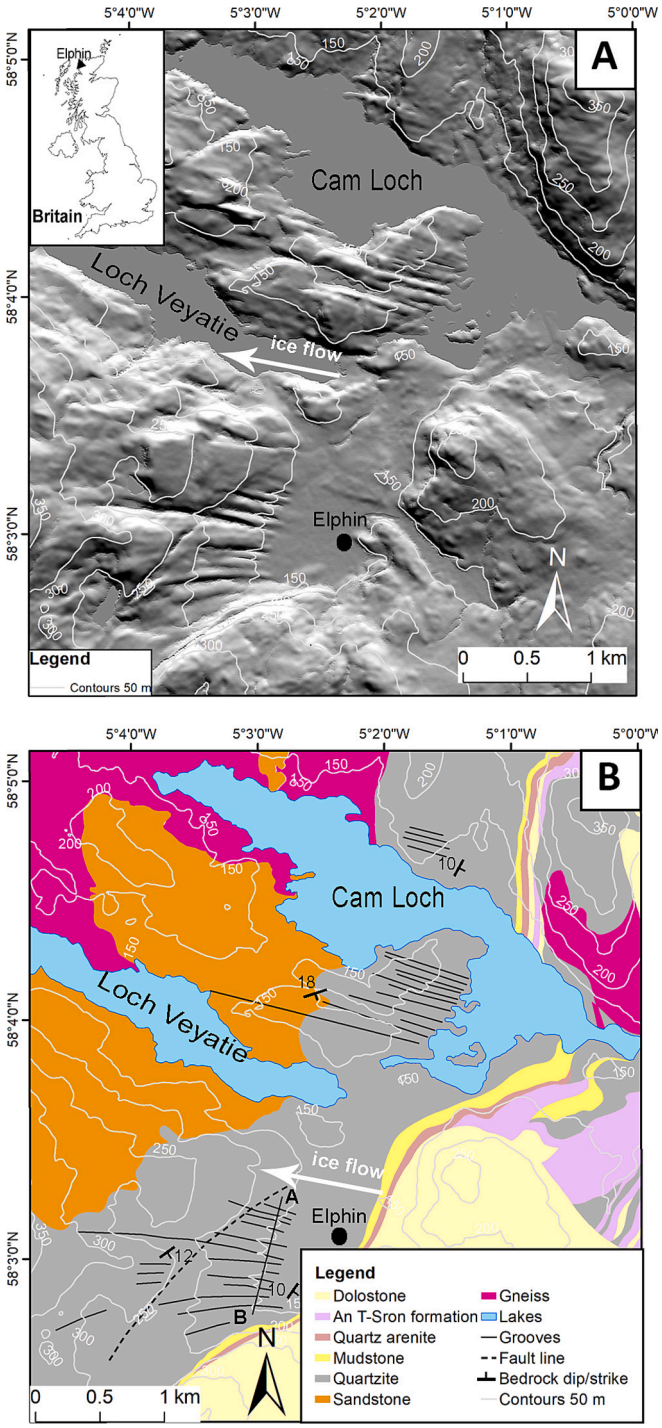

Fig. 6. The Elphin study site: A) Hill-shaded relief NEXTMap digital terrain model showing the grooved terrain west of Elphin village in Assynt, Northwest Highlands of Scotland, UK. Illumination angle at 45° from the north. Inset shows the site location in Northwest Scotland, UK; outline of inset map © vemaps.com. Base image © NERC BGS UK; B) Schematic geology map showing the mega-grooves occurrence in quartz, sub-parallel to the palaeo-ice flow direction. Map modified from digital version (DigMapGB_50, 2016, https://digimap.edina.ac.uk/webhelp/digimapsupport/about_1.htm). The bedrock dip and strike was manually transferred here from the geological map Sheet 101 Ullapool bedrock (British Geological Survey, 2008).

3.3. Ullapool

The BMGs at Ullapool cover an area of around 60 km^2 (Fig. 8A) and occur in metasandstone comprising mainly psammitic rocks (Fig. 8B). The rocks were initially deposited as sandstone in the Proterozoic, in a fluviatile environment (Krabbendam et al., 2008) and subsequently subjected to low-grade metamorphism during the Caledonian Orogeny, which led to pervasive recrystallisation, bed thinning, and the development of strong mica foliation (Fettes et al., 1985). The bed thickness is 10–20 cm, and the rocks are cleaved along the bedding planes and are well jointed (Krabbendam and Bradwell, 2011).

The BMGs were first described by Bradwell et al. (2008), who proposed that they were initiated through focused glacial abrasion under fast-ice flow conditions. This was based upon the location of the grooved terrain in a presumed zone of fast-flow onset and at the up-ice end of the Ullapool tributary, which fed into the Minch Ice Stream (Stoker and Bradwell, 2005; Bradwell et al., 2007; see also Section 3.2). Despite this inference, the role of fast-ice flow to BMG formation at Ullapool remains unclear (Newton, 2022), but there is ubiquitous evidence across the area that the BMGs were subsequently modified by lateral plucking (Krabbendam and Bradwell, 2011; Fig. 9A). Block dislocation through plucking was enabled by the existence of bedrock joints, namely one along the bedding planes and foliation, dipping to the south-east at shallow angles of 12–19°, and two defined by sub-vertical joint systems (J1 and J2 in Fig. 9B; see also Krabbendam and Bradwell, 2011 and Newton, 2022).

Typically, the plucked rock faces have a fresh aspect, with smooth surfaces and sharp edges, and sometimes the dislocated blocks are present close to the place of dislocation (Fig. 9B). Abrasion occurs in the form of rounded edges to strata outcrops rather than glacial striations, the latter having likely been removed through post-glacial weathering and erosion. Striations with a general east–west alignment are abundant on other lithologies along the same flow corridor (Lawson, 1996; Krabbendam and Glasser, 2011), which confirms BMG alignments parallel to former ice flow direction. The Ullapool BMGs have a stair-case profile that is characteristic of grooves in layered rocks (Krabbendam and Bradwell, 2011; Krabbendam et al., 2016), where the shallow groove flank typically corresponds to the bedrock dip plane (Fig. 9A) and the steep flank was developed along sub-vertical joints.

3.4. Franklin

These mega-grooves are located on the western flank of the Franklin Mountains Range, in the lee of a WNW palaeo-ice flow direction (Fig. 10A). Franklin is the most easterly site described by Smith (1948), where BMGs up to 60 m deep occur in the Bear Rock formation, the deepest BMGs reported anywhere onshore (Newton et al., 2018 and Table 1 therein). The Bear Rock formation is the lower member in the Devonian stratigraphy (Fig. 10B), consisting of brecciated limestone with a rubbly, massive structure (Fallas, 2013) and prone to water dissolution, as indicated by widespread karst landforms (Hamilton and Ford, 2002). Although BMGs are deeply incised in the Devonian limestone, they are relatively shallow (1–5 m deep) in the Cretaceous sedimentary rocks where they reach 1–2 km in length (Fig. 10B; Smith, 1948). The Cretaceous sequence consists of soft mudstone, shale and sandstone (Fallas, 2013). Some mega-grooves show continuity when crossing lithological boundaries between Devonian and Cretaceous strata but are mostly discontinuous across the Devonian limestone and Bear Rock formation boundaries (Fig. 10B). The BMGs are aligned on the dip slope of an anticline perpendicular to bedrock strike and at an angle to other major structural lines, such as faults (Fig. 10B). Although not recorded on the geological maps consulted for this study, medium-scale structural features, such as fractures and joints, are typically present in Cretaceous rocks and Devonian sedimentary rocks located west of the Franklin Ridge (Tassonyi, 1969; see also Section 3.4), which would have enabled glacial plucking (see Sections 3.2 and 3.3).

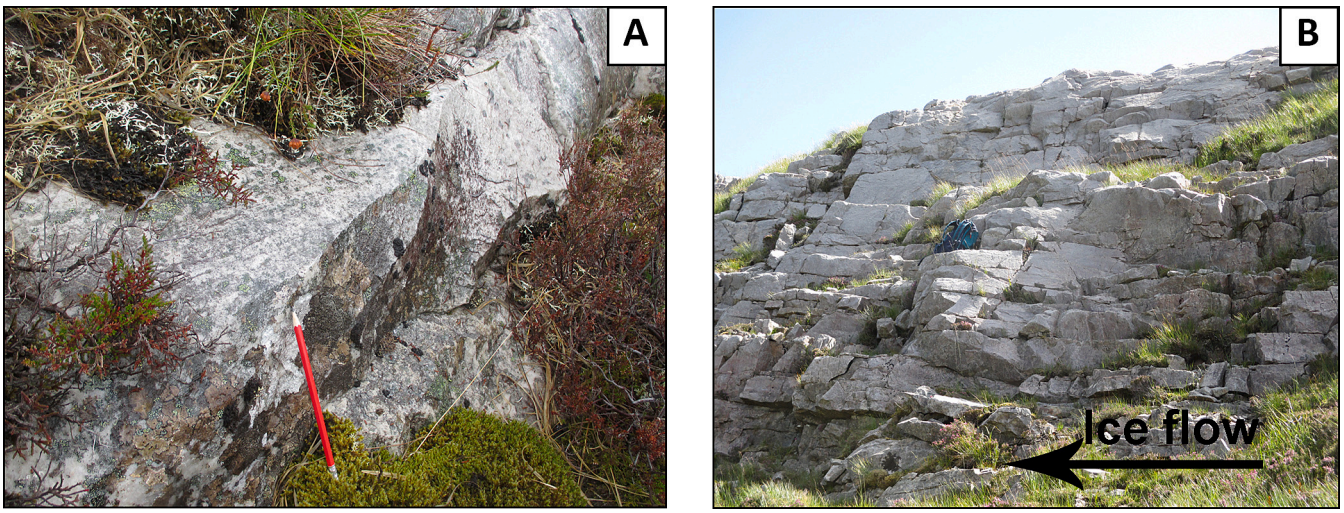

Fig. 7. Field details at the Elphin study site. A) Small-scale evidence of meltwater erosion in the form of shallow cavities with sharp edges; B) plucked debris in a groove flank. The photographs were taken during the fieldwork campaign in the summer of 2018.

Regarding the palaeo-glaciology, there is some uncertainty as to whether ice flow was through streaming or slower, non-streaming ice sheet flow conditions. The palaeo-glacier east of the Franklin Mountains has been interpreted as a branch of the Great Bear Ice Stream (Margold et al., 2015), based upon its location and characteristic streamlined bedform imprint, mostly in unconsolidated sediment (Brown et al., 2011; Brown, 2012; Margold et al., 2015). West of the Franklin Mountains the streamlined terrain is composed of BMGs rather than MSGLs, which occur over large but discontinuous areas. In addition, the BMGs trend in a general NNW direction, being broadly parallel to the Mackenzie River valley (Smith, 1948), and at an angle of approximately 45° to the inferred flow direction of the Great Bear Ice Stream (Fig. 10A; Margold et al., 2015). Although ice streaming cannot be ruled out, a degree of uncertainty remains over the exact nature of the ice flow regime at Franklin.

3.5. Hanna

The site is referred to as "East Mountain" by Hume (1954) and Tassonyi (1969) and as "Site J" by Smith (1948), but here is named after the adjacent Hanna River (Fig. 11A). Hanna is the westernmost site described by Smith (1948), who noted that the grooves occur in fossiliferous Devonian limestone (Fig. 11B) and also that they change their alignment from ESE–WNW to SE–NW (Fig. 11C), which he attributed to a change in ice flow direction. The ice flow direction was up-slope, and the grooves occur on the southern flank of an anticline and are aligned sub-parallel to its east-west trending axis (Fig. 11B).

The BMGs are confined to the Ramparts Formation, of middle Devonian age (Fig. 11B), consisting of two members of marine limestone: the lower Platform Member comprises well-bedded strata, and the upper Reef Member is coralline and more massive (Tassonyi, 1969). The Ramparts Formation in and around the study site comprises both the well-bedded and jointed limestone interbedded with shale, as well as the more massive and porous coralline beds (Hume, 1954 and references therein to unpublished Canol Reports). Albeit speculative, it could be regarded that the change in mega-groove orientation noted by Smith (1948; Fig. 11C) reflects a stratigraphic boundary between the two members, rather than a change in the ice-flow direction. Considering the inferred bed thickness for the Ramparts Formation of 1.2–3.6 m (McLaren, 1962), a conservative expectation is that the joint spacing equals the bed thickness (Fossen, 2016 and Fig. 8.13 therein), which could be regarded as a minimum boundary value for the dimensions of any glacially-plucked debris. Collectively these observations point to geological control over BMG formation at Hanna, with systematic plucking likely to have occurred as it did at Elphin and Ullapool. The inferred palaeoglaciological conditions are of slow, ice-sheet flow, considering the absence of a palaeo-ice stream landsystem and a considerable distance (ca. 200 km) to the nearest reconstructed palaeo-ice stream (c.f. Margold et al., 2015).

3.6. Beavertail

The Beavertail Range is located ca. 12 km north of the Hanna site. The grooves occur on the north-western flank of the Beavertail Range, on the lee side relative to the palaeo-ice flow direction (Fig. 12A). The grooves were mapped by Duk-Rodkin and Hughes (1993) as prominent landforms with a thin veneer of till (0–2 m), which likely conforms to the bedrock topography. BMG alignment to the north-west is consistent with the regional ice-flow direction as well as with the alignment of other BMGs documented in the wider area (Smith, 1948), which supports the subglacial origin of the BMGs at Beavertail. The grooves are located on the dip slope of the Beavertail anticline flank, perpendicular to the bedrock strike (Fig. 12B) and are independent of major geological structures. They occur in the Reef Member of the Ramparts Formation, comprising both coralline, more massive rocks, as well as harder and bedded limestone (Hume, 1954), which suggests favourable conditions for both abrasion and plucking, possibly aided by chemical dissolution, considering the calcareous nature of the rocks. The area was glaciated multiple times during the Quaternary, considering its location in Arctic Canada (Duk-Rodkin et al., 2004; Batchelor et al., 2019; Evans et al., 2021b), but no ice streaming has yet been inferred at Beavertail, and the grooved terrain is a rather isolated occurrence (Fig. 12A). It is therefore assumed that the palaeoglaciological conditions were of normal but sustained ice sheet flow.

3.7. Iivaara

The mega-grooves at Iivaara are located in eastern Finland, on a lee-side slope relative to the palaeo-ice flow direction (Fig. 13A). The landforms were included in the Kuusamo ice lobe complex (Punkari, 1980), and later interpreted as part of a Kuusamo palaeo-ice stream (Sutinen et al., 2010). The grooves are interpreted to have formed through glacial erosion and they lack any structural control (Sutinen et al., 2010).

The site is underlain by an igneous alkaline complex comprising syenite, present within the gneissic parent rock (Geological Survey of Finland, 2016; Fig. 13B). Outside the alkaline complex, on the gneissic parent rock, the landforms are mostly large and widely spaced flutings,

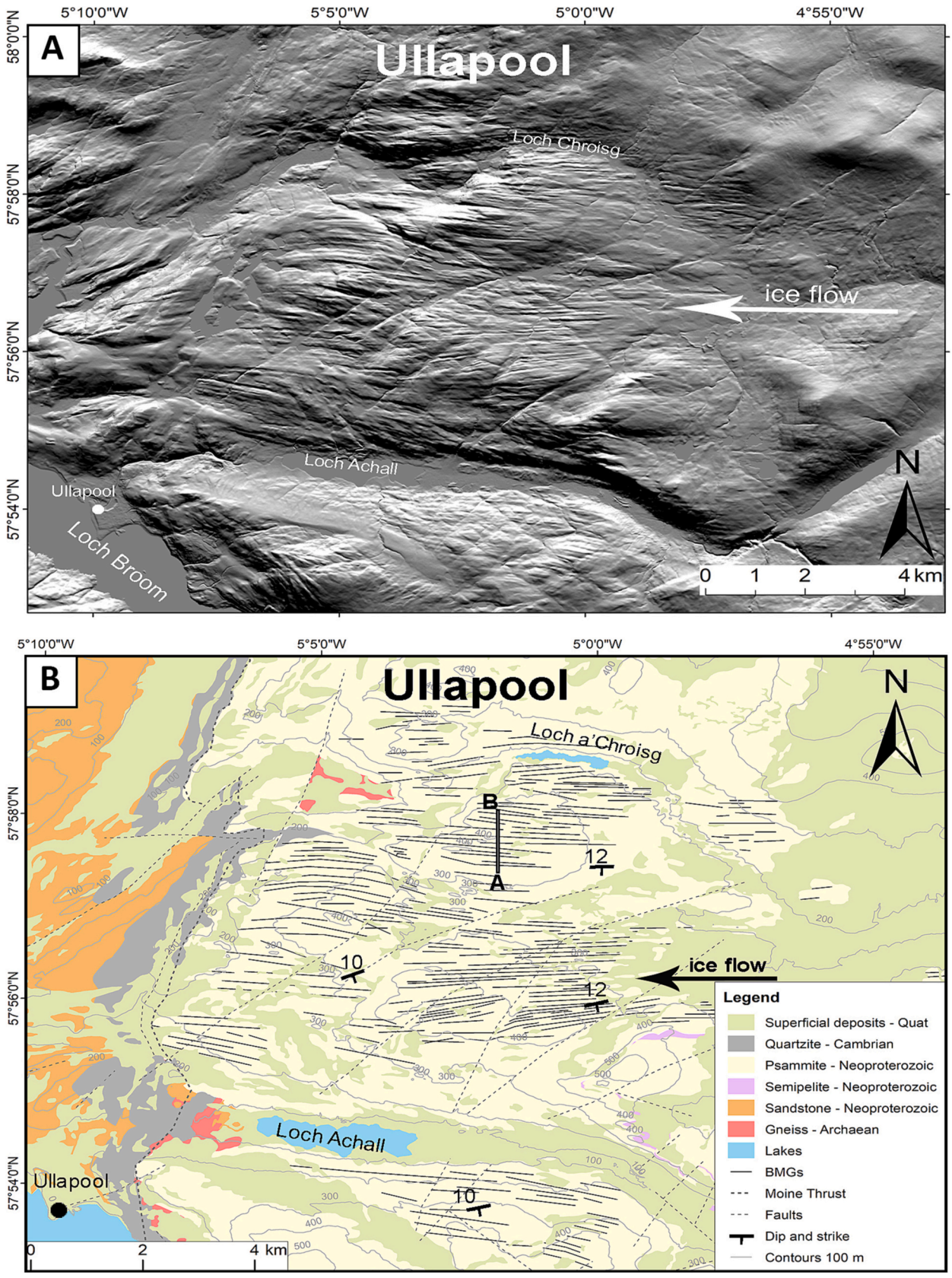

Fig. 8. The Ullapool study area. A) Hill-shaded relief NEXTMap digital terrain model showing the grooved terrain north-east of Ullapool in Assynt, Scotland, UK. Illumination angle at 45° from the north-west. Inset shows location of the Ullapool site in NW Scotland, UK; outline of inset map © vemaps.com. Base image © NERC BGS UK. B) Simplified map of bedrock geology. The dip and strike of the bedding planes was manually digitised from the geological map Sheet 101 Ullapool bedrock (British Geological Survey, 2008). Map modified from digital version of geology map (DigMapGB_50, 2016 https://digimap.edina.ac.uk/webhelp/digimapsupport/about_1.htm).

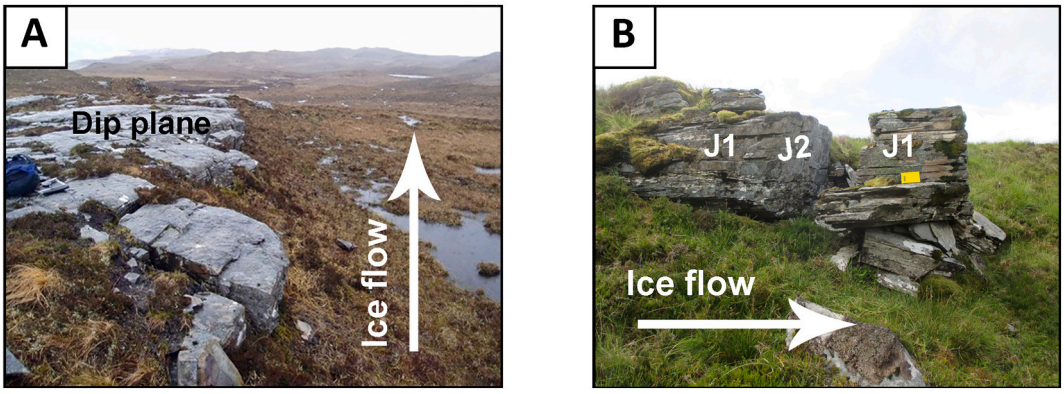

Fig. 9. Field details at the Elphin study site: A) Plucking along the edge of a groove. Note the zig-zag profile of the groove edge. Photo M Krabbendam © NERC, UK. B) psammite block dislocated through plucking southeast of Loch a'Chroisg. The plucked rock has been dislocated along the sub-vertical joint planes J1 and J2, perpendicular to each other, and the bedding plane on which the yellow field book is resting. The photographs were taken during the fieldwork campaign in the summer of 2018. (For interpretation of the references to colour in this figure legend, the reader is referred to the web version of this article.)

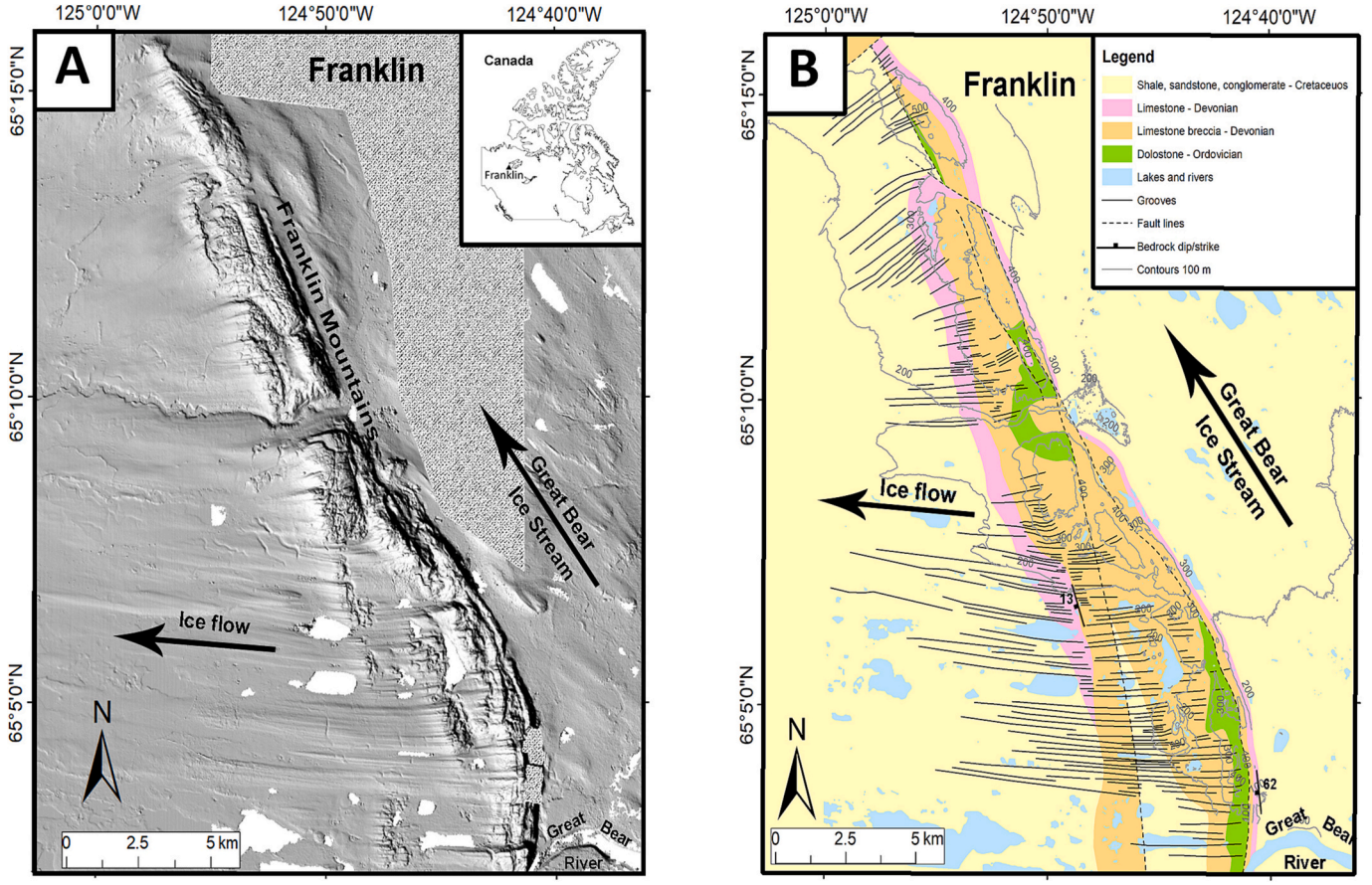

Fig. 10. The Franklin study site: A) Digital elevation model (Arctic DEM) of the grooved terrain at Franklin Mountains, Northwest Territories, Canada. The site lies halfway between the southwest termination of the Great Bear Lake and the Mackenzie River, and the Franklin Mountains ridge is traversed by the Great Bear River. Textured fill represents data voids on the Arctic DEM due to data collection methods (see Section 2.1) and the white areas are lakes or rivers. Illumination angle at 45° from the south. Inset shows location of the Franklin site in the Northwest Territories, Arctic Canada. Outline of inset map © vemaps.com; B) Schematic geology and geomorphology map showing the mega-grooves and the main rock units. The Devonian limestone breccia is commonly referred to as the Bear Rock Formation. The geology map was simplified from Fallas (2013).

in contrast to the narrow and closely spaced BMGs at Iivaara (see Fig. 2 in Sutinen et al., 2010), which suggests a geological control over landform development. The alkaline complex at Iivaara is petrographically heterogeneous on a micro-scale (millimetre to centimetre), comprising rocks of different mineralogy separated by a dense and chaotic network of cross-cutting mineral veins (Lehijärvi, 1960; Sindern and Kramm, 2000; Fig. 13C). The bedrock structure and the relationship between different types of rocks and minerals remain poorly understood in this area (Lehtinen et al., 2005). It is difficult to establish the prevailing mechanism of BMG formation in the absence of detailed field evidence, but considering the lack of bedding, the chaotic spatial arrangement of the mineral veins and the small scale of petrographic heterogeneities,

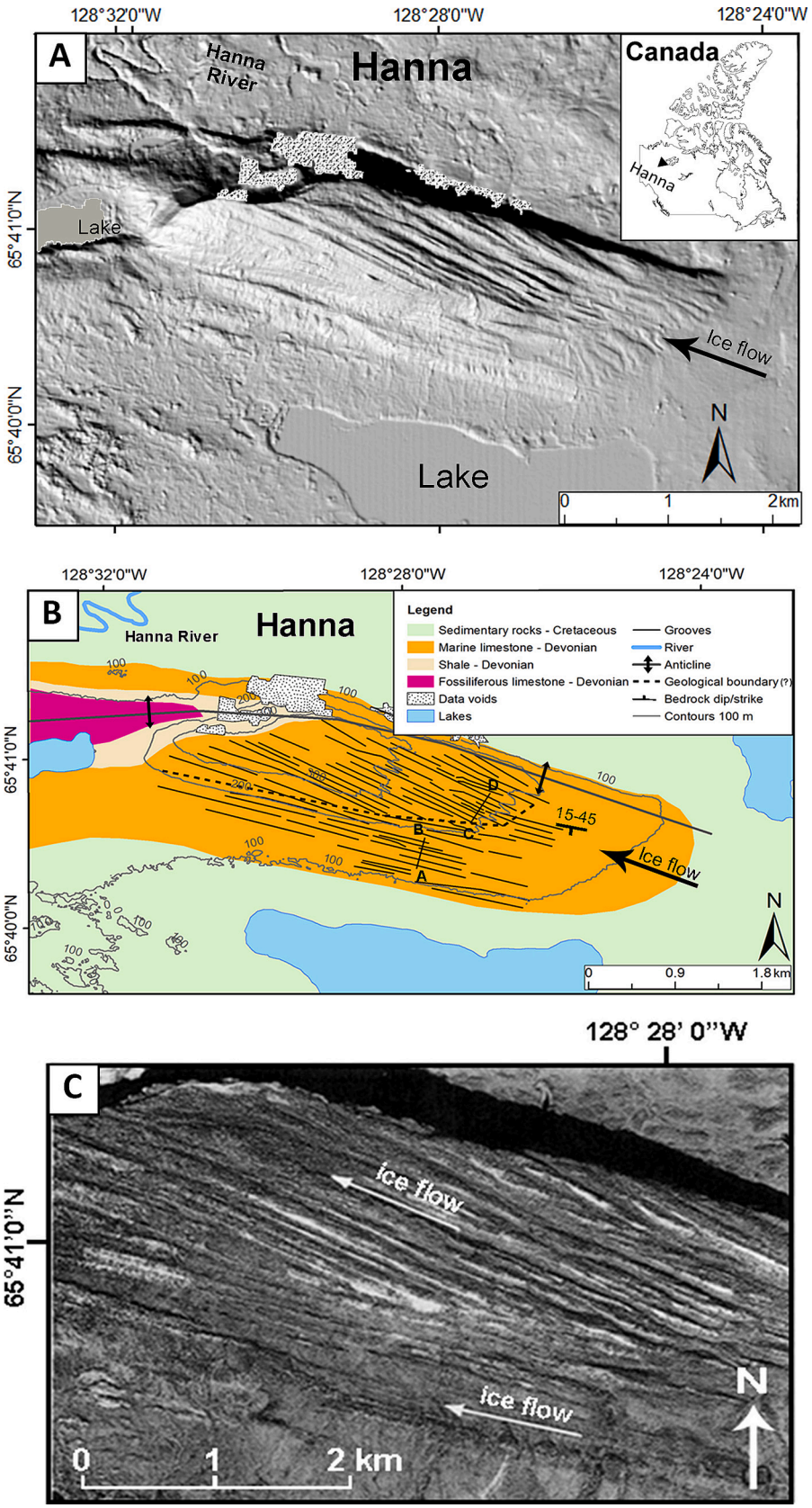

Fig. 11. The Hanna study site: A) Digital elevation model (Arctic DEM) of the grooved terrain at Hanna, Northwest Territories, Canada. Illumination angle at 45° from the north-east. Textured areas represent data voids due to data collection methods (see Section 2.1). Inset shows location of the Hanna site in the Northwest Territories, Canada. Outline map © vemaps.com; B) Schematic geological map showing BMG occurrence in the marine Devonian limestone. The geology map was manually digitised and simplified from Aitken and Cook (1979); C) Aerial photograph of the Hanna site modified from Smith (1948) and reproduced with permission from the American Journal of Science. The white arrows show the two different orientations of the mega-grooves, attributed by Smith (1948) to different ice-flow directions. Base image © *RCAF*.

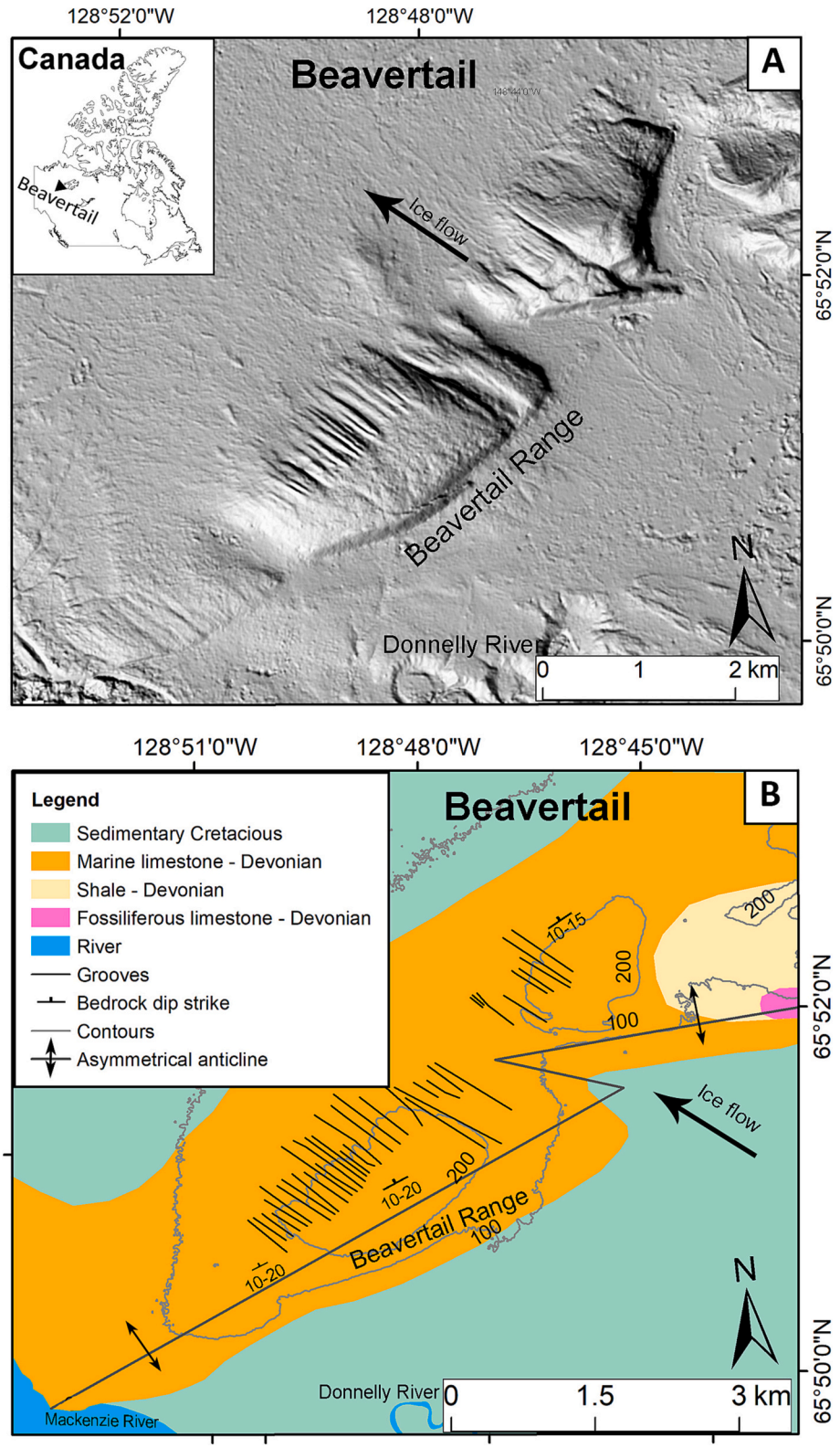

Fig. 12. The Beavertail study site: A) Digital elevation model (Arctic DEM) of the grooved terrain at Beavertail, Northwest Territories, Canada. Illumination angle at 45° from the north-east. Inset shows location of the Beavertail site in the Northwest Territories, Canada. Outline of inset map © vemaps.com; B) Schematic geological map showing the megagroove occurrence in the context of the bedrock geology. The geology map was manually digitised and simplified from Aitken and Cook (1979).

systematic plucking (*sensu* Krabbendam and Bradwell, 2011) is unlikely to have occurred or failed to dislocate large enough rock fragments to have contributed substantially to BMG modification. This geological context offers reduced scope for structural control over BMG formation and points instead to a higher likelihood of glacial abrasion. The latter could have been aided by the transportation of hard-wearing erodents derived from the shield lithology up-flow (Evans et al., 2023).

3.8. Vikna

The BMGs at Vikna are situated offshore, on the Norwegian continental shelf (inset in Fig. 14A). Typically, the inner shelf is composed of Precambrian metamorphic rocks, whereas the mid-shelf consists of younger sedimentary rocks of Palaeozoic and Mesozoic age, with the strike broadly parallel to the coastline (Bugge et al., 1984). At Vikna, the

Table 3
P-values indicative of the degree of statistical significance for the plotted metrics in Fig. 18. Note the frequent occurrence of $p < 0.05$ in the width/depth regression (shaded cells), indicative of statistical significance for the relationship between these two metrics. L = length; D = depth; W = width. The p-values correspond to Figs. S7–S9 in Supplementary Information 1.

Site	Haarefjord	Elphin	Ullapool	Franklin	Hanna	Beavertail	Iivaara	Vikna	Hazelton	Pine Isl	All
L/W	0.005	0.064	0.345	0.3	0.005	0.545	0.166	0.369	0.936	0.041	3.6E−10
L/D	0.030	0.087	0.08	0.467	0.003	0.377	0.481	0.687	–	0.685	0.548
W/D	0.001	0.0003	0.0003	0.0001	5.4E−07	1.22E−06	4.7E−07	0.447	–	0.001	1.3E−22

lithological units have been inferred based on the changes in the general aspect of the topography (Fig. 14A and B). The grooving becomes more attenuated towards the west, possibly due to the presence of thicker unconsolidated sediment (Fig. 14B).

The BMGs occur in the fast-flow onset zone of the Sklinnadjupet palaeo-ice stream (Fig. 14C), one of the numerous ice streams that drained the Fennoscandian Ice Sheet to the west during the last deglaciation (Ottesen et al., 2005). Palaeo-ice stream reconstructions on the Norwegian continental shelf were based on the characteristic streamlined bedrock forms closer to the fast-flow onset zone, followed to the west by long trains of MSGLs in unconsolidated sediments stretching across the outer continental shelf (Ottesen et al., 2002). The Sklinnadjupet ice stream flowed to the north-west and formed a large streamlined bedform assemblage down-flow from the Vikna grooves (Ottesen et al., 2005). Seismic profiles show that the grooves at Vikna were eroded in bedrock (Fig. 14D). The geological and palaeoglaciological scenario at Vikna is similar to that in Ontario, Canada, where the Huron palaeo-ice stream initiated its fast flow over the gneissic bedrock of the Canadian Shield and flowed westwards over the Palaeozoic sedimentary bedrock, where it produced streamlined bedforms, including BMGs (Eyles, 2012; Krabbendam et al., 2016).

3.9. Hazelton

The BMGs here occur on the south-western flank of the Hazelton Ridge of the Canadian Rockies, on the lee side relative to the regional palaeo-ice flow direction (Fig. 15A) and have been eroded in sedimentary rocks of the Lower Cretaceous formations, along the dip planes, subperpendicular to the bedrock strike (Fig. 15B). The rocks consist of sandstone, siltstone and mudstone (Evenchick et al., 2008). The BMGs, previously assigned a glacial origin by Krabbendam et al. (2016), have recently been interpreted as part of a wider streamlined bedform assemblage formed by the Skeena Ice Stream (Eyles et al., 2018). The Skeena Ice Stream was a land-terminating ice stream which flowed southwards in the British Columbia Cordillera and left a rich archive of streamlined bedrock forms along the main valleys and across high-altitude plateaus, as well as MSGLs in the lowlands outside the mountainous area (Eyles et al., 2018). In the absence of empirical evidence pertaining to the BMGs, or a more detailed relationship to geological structure, it is difficult to assess the main mechanism of erosion responsible for their formation. However, sedimentary Cretaceous strata typically consist of bedded rocks, with beds of varying thickness and hardness (Evenchick et al., 2008), which likely enabled glacial plucking.

3.10. Pine Island

The Pine Island study area is situated on the inner West Antarctic continental shelf, relatively close to the current ice margin (Fig. 16A) and comprises grooves and streamlined ridges interpreted as being formed through a combination of glacial erosion and subglacial meltwater under ice-streaming conditions (Lowe and Anderson, 2002 and 2003). Meltwater is regarded as an important erosive agent on the ice stream bed at Pine Island, with the recognition of a huge anastomosing system of large-scale bedrock channels upstream from the grooved terrain, thought to have formed through rapid erosion following subglacial lake outbursts (Kirkham et al., 2019). The Pine Island glacier has repeatedly advanced and retreated during the late Quaternary (Graham et al., 2010) and its bed has been identified as an area subject to intense erosion upstream from the grooved area (Smith et al., 2012). The palaeo-ice stream at Pine Island has left a clear geomorphic signature in the substrate, with BMGs being a common occurrence in the upper part of a palaeo-ice stream landsystem, alongside other bedrock forms elongated in the ice flow direction, including canyons, rock drumlins and crag-and-tails (Lowe and Anderson, 2003). Geophysical investigations indicate a substrate of crystalline bedrock, with unconsolidated deposits forming a thin and patchy cover, which supports groove occurrence in bedrock. Collectively, the evidence strongly suggests a glacial origin for the BMGs, which formed through bedrock erosion under sustained fast-ice flow conditions (Fig. 16).

4. Results

4.1. BMG metrics

The summary statistics for length, width, depth, spacing, elongation and azimuth were calculated in Excel (Supplementary Information 2) and the results are presented in Table 2. The frequency distributions for the overall populations are illustrated in Fig. 17. The site-specific spatial distribution for each metric is presented in Figs. S2–S6 in Supplementary Information 1. Upper and lower values at the 10th and 90th percentile are reported rather than the minimum and maximum, to avoid data skewing by extreme values that may have been unrepresentative (cf. Spagnolo et al., 2014). The value ranges for individual sites are represented in the box plots in Fig. 17A–E.

Dimensions for most BMGs are as follows:

- length 220–2270 m (mode 400–500 m, median 662 m; Table 2; Fig. 17A),
- width 21–210 m (mode 200 m, median 76 m; Table 2; Fig. 17B),
- lateral spacing 35–315 m (mode 84 m, median 95 m; Table 2; Fig. 17C),
- depth 2–15 m (mode 3 m, median 5 m; Table 2; Fig. 17D).
- elongation ratios 5:1–41:1 (a mode of 8:1–10:1, median of 15:1; Table 2; Fig. 17E).

The deepest grooves occur at Pine Island, with a median of 14 m, which is double the median range of 2–7 m for all the other sites (Table 2; Fig. 17D). The highest values for length, width and spacing

occur at Vikna and Pine Island, whereas the lowest values apply to BMGs at Iivaara, Hazelton and Haarefjord (Fig. 17A–C). This hierarchy is reversed for elongation ratios, with the highest values at Haarefjord (mean 42:1), and lowest values at Vikna (mean 5:1) and Pine Island (mean 7:1; Fig. 17E). At most sites, the azimuth of the BMGs has a low standard deviation of 4–8° (Table 2), indicative of a strong parallel conformity between grooves within individual sites. The mean azimuth value coincides with that of the regional ice-flow direction inferred from independent evidence (see Section 3), which confirms the empirical observations that BMGs are aligned parallel to former ice flow. Relatively high values for azimuth standard deviation are 14° at Franklin and 22° at Hanna (Table 2), indicative of a change in BMG alignment within these sites. At Franklin, BMG alignment changes from westwards to north-westwards (Fig. 10). At Hanna there are two slightly divergent orientations for the BMGs (Fig. 11C), likely due to changes in the geological structure (see Section 3.5). BMG density, calculated as number of landforms per unit area, was highest at Iivaara and Haarefjord (>30/km^2), and lowest at Vikna and Pine Island (<2/km^2; Table 2).

4.2. Relationships between BMG dimensions

The relationships between metrics based on values derived from the overall sampled BMGs, across the global dataset, show a positive linear trend, albeit generally weak, as indicated by the low R^2 values of 0.001–0.321 (Fig. 18). The relationships between length and other metrics yield the weakest positive trends both across the global population, as suggested by $R^2 < 0.13$ (Fig. 18A and C), as well as within individual sites (Figs. S7 and S8 in Supplementary Information 1). In practical terms, this indicates that the widest and deepest BMGs can be either short or long. The strongest correlation ($R^2 = 0.32$) is that between width and depth (Fig. 18C), likely indicating that BMGs consistently grow wider as they get deeper. This relatively strong correlation between groove width and depth remains apparent at all individual sites and is always statistically significant ($p < 0.05$; Table 3; Fig. S9 in Supplementary Information 1; see Section 5.5). However, the overall weak relationships between BMG metrics point to a high variability in the local factors which control BMG evolution (see Section 5.3).

To examine whether various metrics might be related to or associated with processes governing BMG evolution across sites and also to enable comparisons of BMG metrics between sites, the relationships between length, width, depth and spacing were explored in combinations of two metrics. The plotted figures in Fig. 19 represent site-specific values for these metrics, calculated as overall mean values for the sampled BMG population within each individual site. Each plot is fitted with a linear trendline. All relationships show strong positive trends with $R^2 = 0.4$–0.9 and all are statistically significant, as reflected by the p-values < 0.05 (Fig. 19).

The correlations between length and all the other metrics are positive and strong, as reflected in the high $R^2 = 0.7$ (Fig. 19A–C). The almost perfectly linear relationship between width and spacing ($R^2 = 0.9$; Fig. 19D) needs to be treated with care because the two metrics co-vary and are therefore not independent. This is because two adjacent grooves need to merge for spacing between grooves to grow, which would result in the formation of a wider groove. If this is replicated across the population at any site, the resulting mean values for both width and spacing would therefore increase. The width/depth and spacing/depth relationships with R^2 values for the linear trends lying at 0.4 and 0.5, respectively, also support a convincing positive correlation between those metrics, albeit somewhat weaker than the correlations involving length (Fig. 19E and F).

In order to investigate the efficiency of erosion processes, the variations in width and depth along the grooves were plotted in the down-ice direction and the graphs fitted with a linear trendline (Fig. 20A and B). The results show different trends between sites, which can be either positive or negative, but there is usually consistency within the same site between the variation of depth and that of width with flow distance down-ice. Thus, at Elphin, Ullapool and Hanna the trends are positive, showing that BMGs widen and deepen along the ice-flow direction, whereas Franklin, Iivaara, Vikna and Pine Island have downward trends, showing that BMGs become narrower and shallower with distance downstream.

In summary, the correlations between metrics derived from BMGs within individual sites are positive, but weak, indicative of a high degree of variability in BMG morphological development within sampled sites. Relationships between overall site-specific mean values show much stronger positive correlations of metrics across the site population, indicative of possible overarching relationships in BMG development. The variations in depth and width along the grooves is positive at some sites and negative at others, but the two trends are usually consistent within individual sites.

5. Discussion

5.1. Comparisons with previous studies

Comparisons between metrics reported here with those reported in previous studies show various degrees of consistency. At Haarefjord there is good consistency between length, width and depth between the value ranges of 10th–90th per centile reported here and the average values reported by Funder (1978). For example, length values as reported by Funder (1978) are 50–2000 m, compared with 142–1203 m in this study (Table 2); widths are 45 m on average (Funder, 1978) and 19–43 m in this study (Table 2); spacing is 45 m on average (Funder, 1978) and 27–62 m in this study (Table 2); depth values reported by Funder (1978) are 1–5 m, compared to 2–7 in this study (Table 2). This consistency may reflect the fact that mapping was done on high-resolution imagery for the same area in both studies. Table 2 At Ullapool and Elphin the values for length, depth and spacing reported here are lower than those of Bradwell et al. (2008) and Bradwell (2005), respectively. Table 2 Metrics differences are likely due to the fact that the area studied by Bradwell et al. (2008) is larger, covering the entire length of the Ullapool tributary glacier, spanning different lithologies with variable susceptibility to erosion (c.f. Krabbendam and Glasser, 2011; Newton, 2022). The area sampled here is confined to the Moine Schists (Fig. 8B), therefore the metrics are representative of this particular type of rock. In addition, there are differences between the two studies in the protocol for groove selection, whereby grooves which occur along structural lines (e.g. faults) were excluded in this study to avoid the results being skewed by structural factors (see Section 2.2).

5.2. Spatial and statistical distribution of BMG dimensions

The frequency distribution patterns of the aggregated dataset are unimodal for all metrics, with no obvious breaks or stepped patterns to suggest separate sub-populations or different scenarios of formation across each site (Fig. 17). In addition, the value ranges for all metrics always overlap, regardless of discrepancies between end members (see Fig. 17). Collectively, these observations imply that, at least morphometrically, BMGs appear to form a single landform population, which justifies their treatment as a distinctive landform type and the use of specific terminology to describe them. The same conclusion has been reached based on similar analyses for other subglacial bedforms, such as drumlins (Clark et al., 2009), ribbed moraine (Dunlop and Clark, 2006), MSGLs (Spagnolo et al., 2014) and eskers (Storrar et al., 2014).

Notably, however, there is marked variation between individual sites in the spatial distribution of BMG metrics. In particular, the range of values is different between sites for the same metric (e.g. Fig. S3 in Supplementary Information 1). The high standard deviation for length reflects the fact that BMGs of very different lengths can occur within most sites. Depth has the lowest standard deviation across the sampled sites, reflecting a strong internal consistency in the development of this

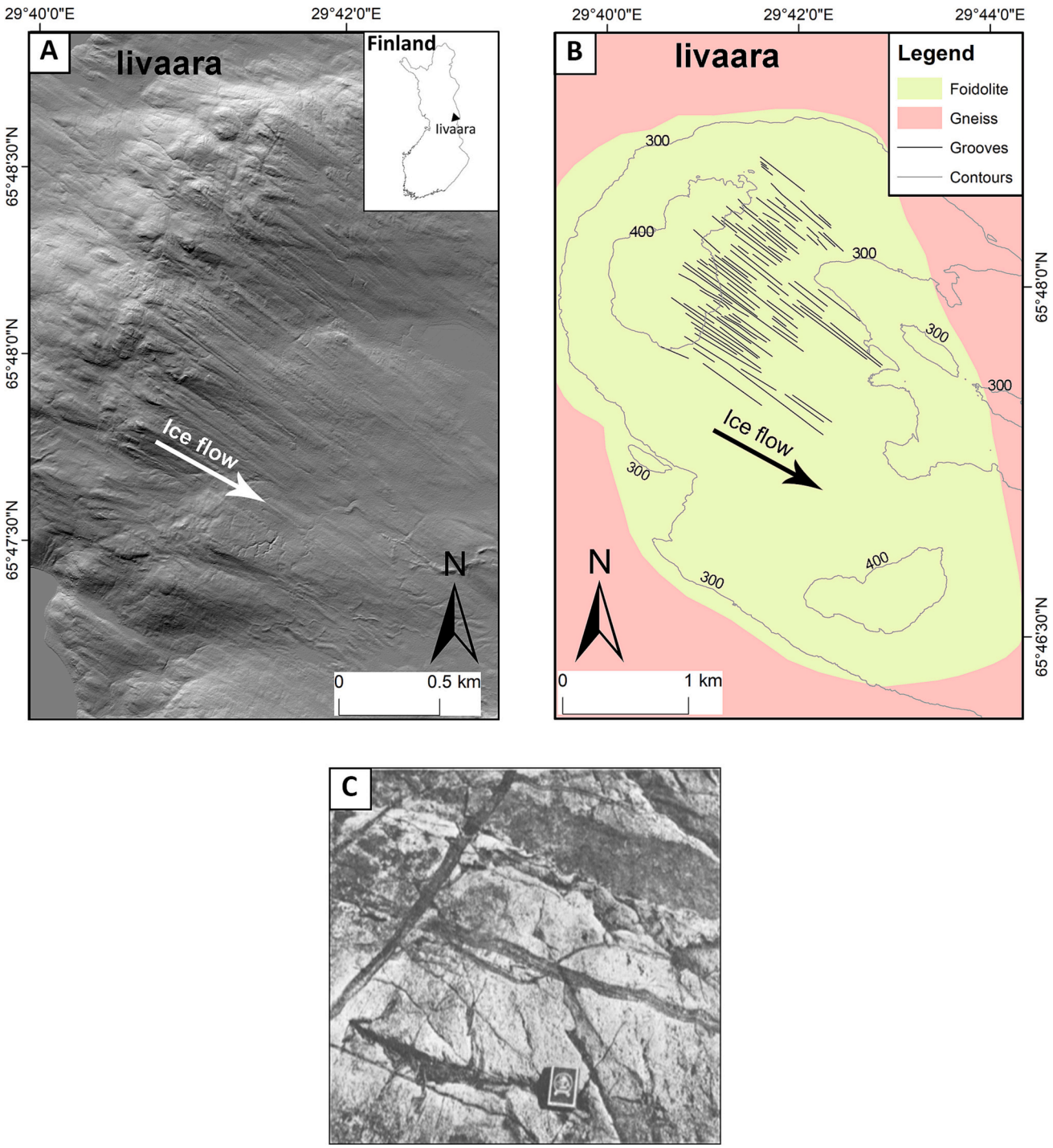

Fig. 13. The Iivaara study site: A) Digital elevation model of the Iivaara site, located in the Kuusamo area, eastern Finland. Inset shows location of the Iivaara site in eastern Finland; outline of inset map © vemaps.com. Base image © National Land Survey of Finland; B) Geological map of Iivaara modified from the GIS database of the Geological Survey of Finland (2016); C) Pyroxene-rich veins criss-crossing the paler rock. Image reproduced from Lehijärvi (1960).

metric, likely dictated by the bedrock-specific susceptibility to erosion. Most frequency distributions at individual sites are unimodal (e.g. Figs. S3–S5 in Supplementary Information 1), whereas some have a less obvious modal value (e.g. Figs. S2–S4 in Supplementary Information 1) which reflects a more evenly balanced presence of BMGs of various dimensions. The skew can be symmetrical, with tails left and right of equal length, so the distribution patterns at individual sites do not consistently mirror those for the aggregated population. In the case of MSGLs, the opposite was noted, in that the frequency distribution patterns of individual sites do mirror those of the aggregated landform population, arguably due to the uniformity of the substrate in unconsolidated sediments (Spagnolo et al., 2014). Overall, the inter-site variability in frequency distributions of BMG metrics is interpreted to reflect a strong influence of local conditions over individual BMG development (see Section 5.3). This variability is also apparent from the weak correlations between metrics, especially those between length/width and length/depth derived from both the aggregated sampled population (Fig. 18A and B) as well as from the sampled BMGs within individual sites (Figs. S7 and S8 in Supplementary Information 1). Nevertheless, despite pronounced local variability in BMG formation, the fact that metrics across

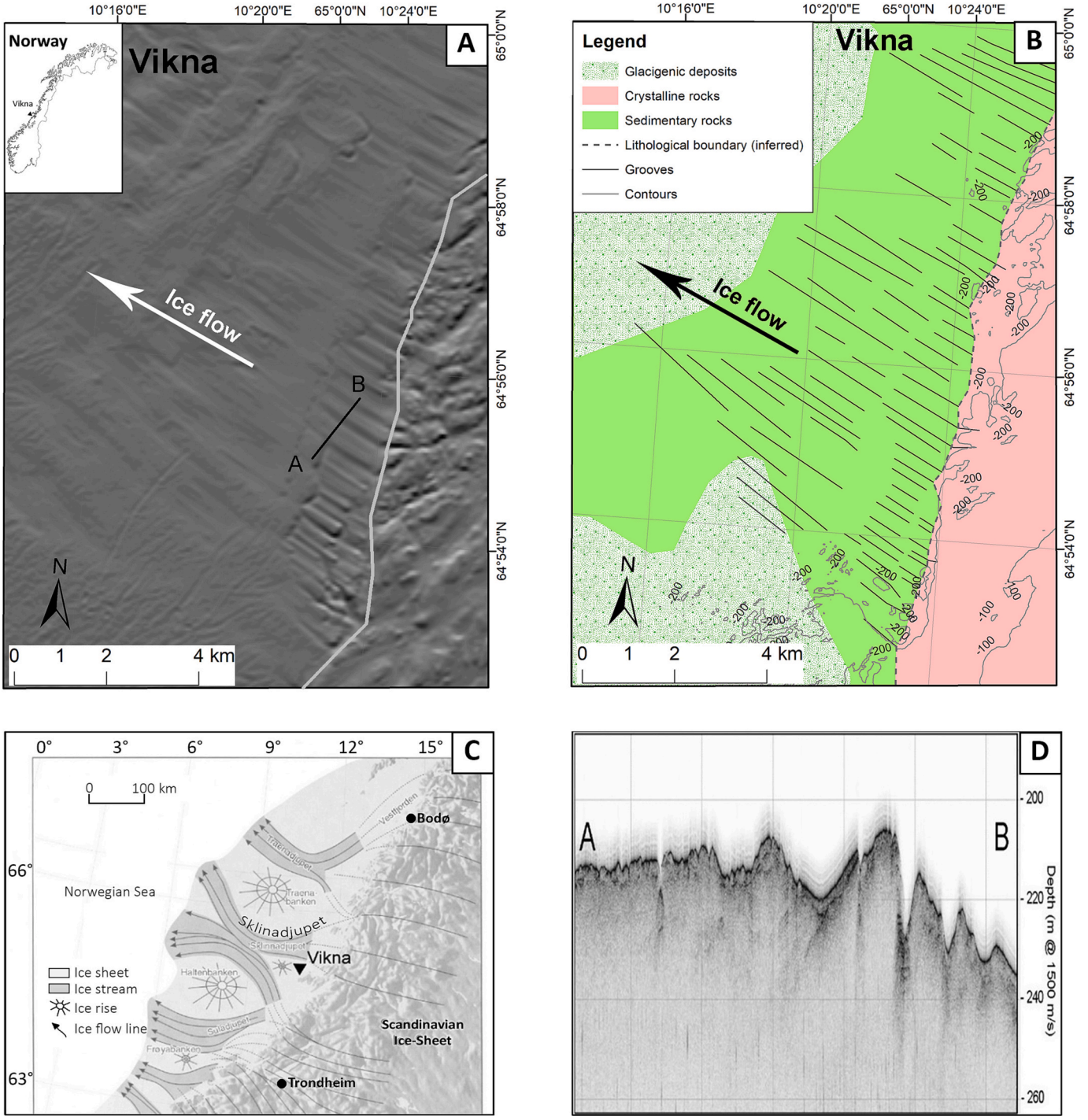

Fig. 14. The Vikna study site: A) Digital elevation model of the Vikna site. The grey line represents the inferred lithological boundary between crystalline and sedimentary bedrock. A–B represents the transect of the seismic profile in Fig. 14D. Inset shows location of the Vikna site in western Norway; outline map © vemaps.com. Base image © Norwegian Hydrographic Service; B) Inferred geological map of the Vikna site; C) Location of the Vikna site in relation to palaeo-ice streams. Image modified from Ottesen et al., 2002. Base image © Geological Society of London; D) Seismic profile at Vikna with substrate aspect showing that the grooves occur in bedrock. Profile transect shown in Fig. 14A. Image courtesy Norwegian Hydrographic Service.

the aggregated global population produce unimodal frequency distributions (Fig. 17) with overlapping value ranges between sites (box plots in Fig. 17) strengthens the conclusion that BMGs represent a single landform population.

In contrast to the weak metrics relationships between sampled individuals, the site-specific, overall mean values for BMG metrics show strongly consistent and positive linear correlations (Fig. 19; see Section 4.2). This is surprising considering the geological differences between sites, the potential differences in glaciological conditions and in landform age, and differences in topography. These strong correlations mean that, regardless of any geomorphic constraints or differences in BMG initiation, the overall evolution of BMG dimensions within any site is quite predictable. Thus, if a site-specific mean value for groove length was known, the equivalent mean value for width, depth and spacing could be estimated within relatively narrow margins of error, based on the equations derived from the trendlines in Fig. 19. These results could

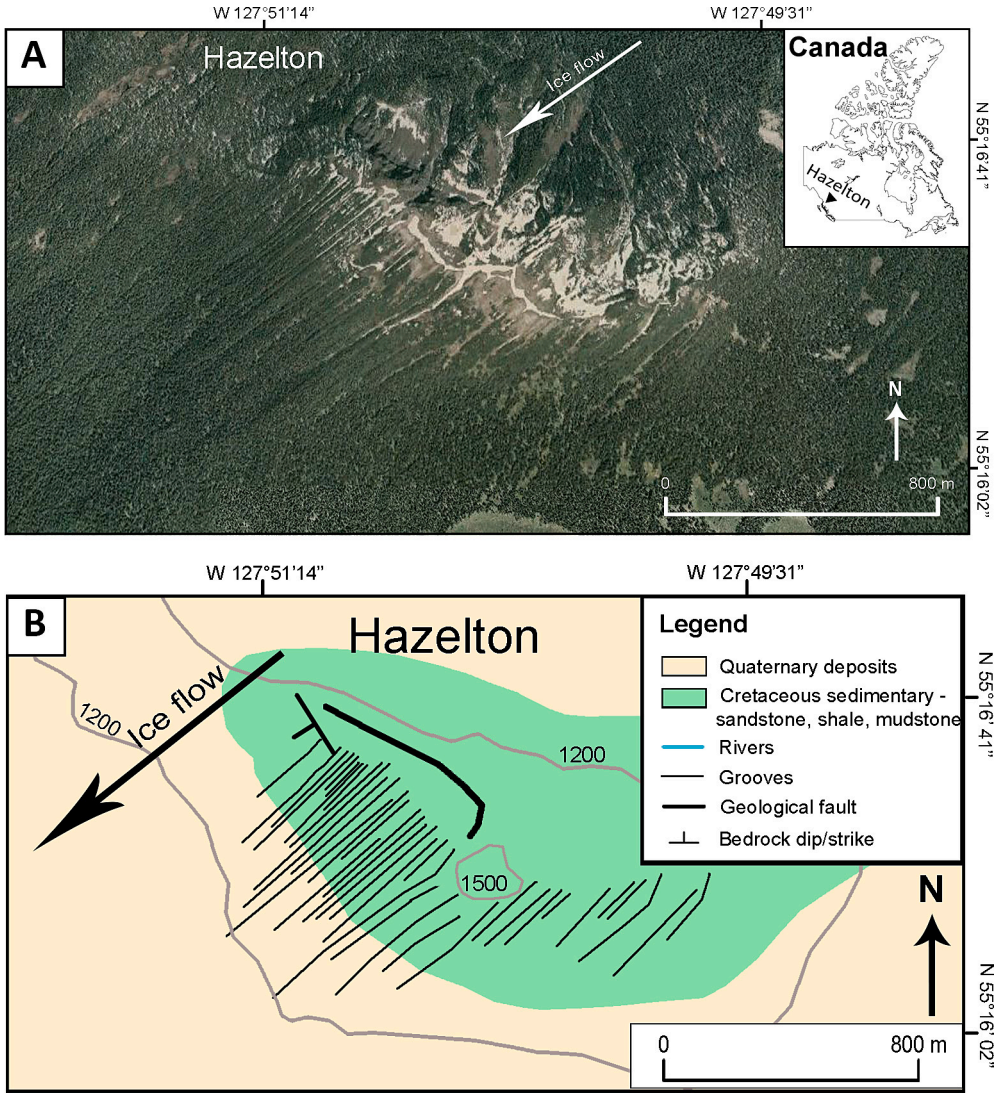

Fig. 15. The Hazelton study site: A) Aerial photograph of the grooved terrain at Hazelton. The site is located west of Skeena River, ca 10 km north-west from New Hazelton town, British Columbia, Canada (image © GoogleEarth Pro); B) Simplified geological map, digitised from Evenchick et al. (2008).

be further refined by reducing potential overestimations of BMG width and depth at Vikna and Pine Island if mapping could be done at higher resolution (see Section 2.2). In principle, modelling experiments could use these results to further explore BMG evolution through time (see also Section 5.5) and further unravel overarching rules that could be governing BMG development (see Evans et al., 2023).

In conclusion, BMGs represent a discreet landform type which, once initiated, seem to develop under an overarching scenario, considering the strong correlations between mean metric values *between* sites. This is despite pronounced local variability in metric correlations manifested *within* individual sites, and despite variations in physical and glaciological characteristics between sites.

5.3. Controlling factors of BMG morphometry: geology versus glaciology

At Vikna and Pine Island, a series of common characteristics of the BMGs point to a primary glaciological control over their development, through enhanced erosion beneath fast-flowing glacier ice. Firstly, both sites experienced a similar glaciological history, with the BMGs being situated on continental shelves in polar regions affected by marine-terminating ice streams during the last glacial, and in zones of fast-flow (Ottesen et al., 2002 and 2005; Lowe and Anderson, 2002 and 2003; Kirkham et al., 2019). Secondly, the value ranges for the BMG metrics are strikingly similar between the two sites, and they stand out in the global dataset at the higher end of the spectrum (Fig. 17A–D). Thirdly, the two sites are underlain by different bedrock geology, namely sedimentary at Vikna (Fig. 14BFig. 12B) and crystalline at Pine Island, with each rock type known to produce its characteristic topography through glacial erosion under slow ice flow conditions. Thus, sedimentary rocks typically enable the formation of streamlined bedrock forms (Eyles, 2012; Eyles and Putkinen, 2014), whereas crystalline bedrock leads to the development of classic cnoc-and-lochan topography, typically with reduced streamlining, common in glaciated shield terrain (Linton, 1963; Sugden, 1974; Krabbendam and Bradwell, 2014). However, at Pine Island, the dominant topography is that of grooved and streamlined bedrock, similar to the crystalline streamlined bedforms in West Greenland, also formed by enhanced abrasion under ice-streaming conditions (Roberts and Long, 2005; Roberts et al., 2010; Roberts et al., 2013). At Vikna, the streamlined topography is not uncommon for the bedrock type, but the BMG dimensions far exceed those of BMGs in similar types of bedrock (e.g. Ullapool, Hanna, Beavertail; Fig. 17).

The elongation ratios for the BMGs at Vikna and Pine Island have the lowest values in the dataset (Fig. 17E) and a strikingly similar unimodal frequency distribution spanning a short range of low values, with similar mode values between the two sites of 4:1–6:1, which differs from those at all other sites (Fig. S5 in Supplementary Information 1). In addition

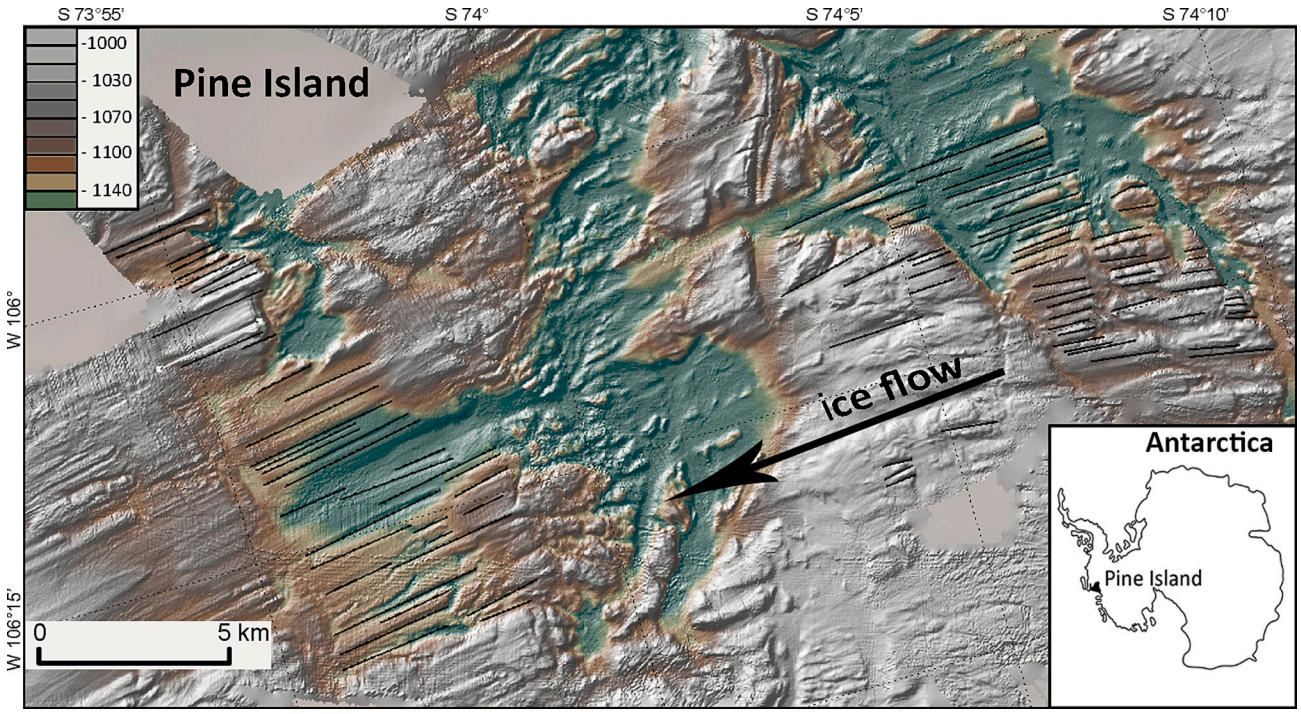

Fig. 16. The Pine Island study site: A) Satellite image of the Pine Island Glacier flowing into the sea at Pine Island Bay, Antarctica. Inset shows location of study area within Antarctica. Image modified from Lowe and Anderson (2002); B) DEM of the grooved site at Pine Island situated on the West Antarctic continental shelf in Pine Island Bay. The units in the colour key represent meters. Base image © GeoMapApp.

this modal value is similar to that for the streamlined gneissic bedrock forms at Jakobshavns, West Greenland (approximately 5:1) from an area also affected by enhanced erosion due to ice-streaming conditions (Roberts et al., 2010). The unimodal frequency distribution of elongation ratios could therefore represent a tendency for scaling (c.f. Clark et al., 2009) following either prolonged subglacial erosion or a relatively short period of efficient lateral erosion beneath fast-flowing ice. In other words, as the BMGs evolve, they may get wider (see Section 5.4), which would be consistent with the low values for groove density at these locations (Table 2). Collectively, the common characteristics of the BMGs from Vikna and Pine Island strongly indicate BMG development under the primary influence of fast-flowing ice, which enabled high rates of subglacial erosion and superseded any geological controls.

Apart from Vikna and Pine Island, the other sampled areas comprise BMGs that have much smaller dimensions, especially with respect to length and width (Fig. 17A–D), whereas elongation ratios and landform density are up to one order of magnitude higher (Table 2). At several of these areas a strong geological control factor in BMG formation was established through direct empirical evidence (e.g. Smith, 1948; Funder, 1978; Krabbendam and Bradwell, 2011 Sections 3.1), or inferred from published geological data (Hume, 1954; McLaren, 1962; Tassonyi, 1969 - see Sections 3.4–3.6; Lehijärvi, 1960; see Section 3.7).

At Elphin and Ullapool it has been established through fieldwork that plucking was the main mechanism that modified the BMGs during the last glaciation, enabled by a dense, three-dimensional network of joints in the bedrock (Bradwell, 2005; Krabbendam and Glasser, 2011; Krabbendam and Bradwell, 2011; Newton, 2022; see Figs. 7B and 9B). Abrasion and meltwater erosion were also operational, but their effects were assessed as minimal considering the shallowness of striations and meltwater-sculpted cavities (Bradwell, 2005; Krabbendam and Glasser, 2011; Newton, 2022; see Sections 3.2 and 3.3; Fig. 7A). The inferred presence of joints and their alignment relative to the BMGs (Hume, 1954; McLaren, 1962; Tassonyi, 1969) indicates that plucking is highly likely at Hanna and Beavertail (see Sections 3.5 and 3.6). At Hanna the BMG alignment parallel to bedrock strike and the two different directions in BMG orientation could indicate structural control over BMG formation (see Section 3.5; Fig. 11C) rather than a change in ice-flow direction (Smith, 1948). Interestingly, the BMGs at all four sites share common characteristics. Thus, the positive correlation between groove depth and width with distance down-flow (Fig. 20) is consistent with plucked rocks becoming entrained into glacial transport and acting as erosive tools further down-ice, leading to groove widening and deepening down-ice flow. Also, BMG density at Hanna, Beavertail and Elphin is similar, lying within a narrow range of 13.5–15.5 landforms/km^2 (Table 2), possibly indicative of groove development under similar constraints. Based on morphometric comparisons between Elphin and Ullapool on the one hand, and Hanna and Beavertail on the other, it is likely that plucking was pervasive at the Canadian sites and constituted the prevailing mechanism of BMG formation there.

At Haarefjord and Iivaara it is thought that abrasion, rather than plucking, was the main mechanism of erosion considering the massive and poorly jointed bedrock (Collinson, 1972; Lehijärvi, 1960; see Sections 3.1 and 3.7; Fig. 13C). At Haarefjord, abrasion was regarded as the primary mechanism of BMG formation by Funder (1978) following landform examination in the field. Significantly, the results of quantitative analyses show close similarities between the grooves at these two sites, consistent with the expected geomorphic outcomes of abrasion (Iverson, 1991; Krabbendam and Glasser, 2011). Thus, the relatively small dimensions of the BMGs at these two sites (Fig. 17) are consistent with low efficiency of abrasion in comparison to plucking, documented in both glacial and fluvial environments (Whipple et al., 2000; Dühnforth et al., 2010). The relatively high groove densities of 31.2 grooves/km^2 at Haarefjord and 43.5 at Iivaara, which is more than double the density at any other site (Table 2), could reflect the reduced effect of lateral plucking, which inhibited groove widening, also consistent with low values for width and spacing (Fig. 17B and C). Furthermore, at Iivaara the grooves become narrower and shallower with distance down-ice (Fig. 20), consistent with the wearing out of abrasive tools with distance downstream, as in the case of striations (Iverson, 1991), supporting the notion that BMGs may essentially be giant striations (Bukhari et al., 2021; Evans et al., 2021a; developed further in Evans et al., 2023). However, attempts to differentiate between the prevalence

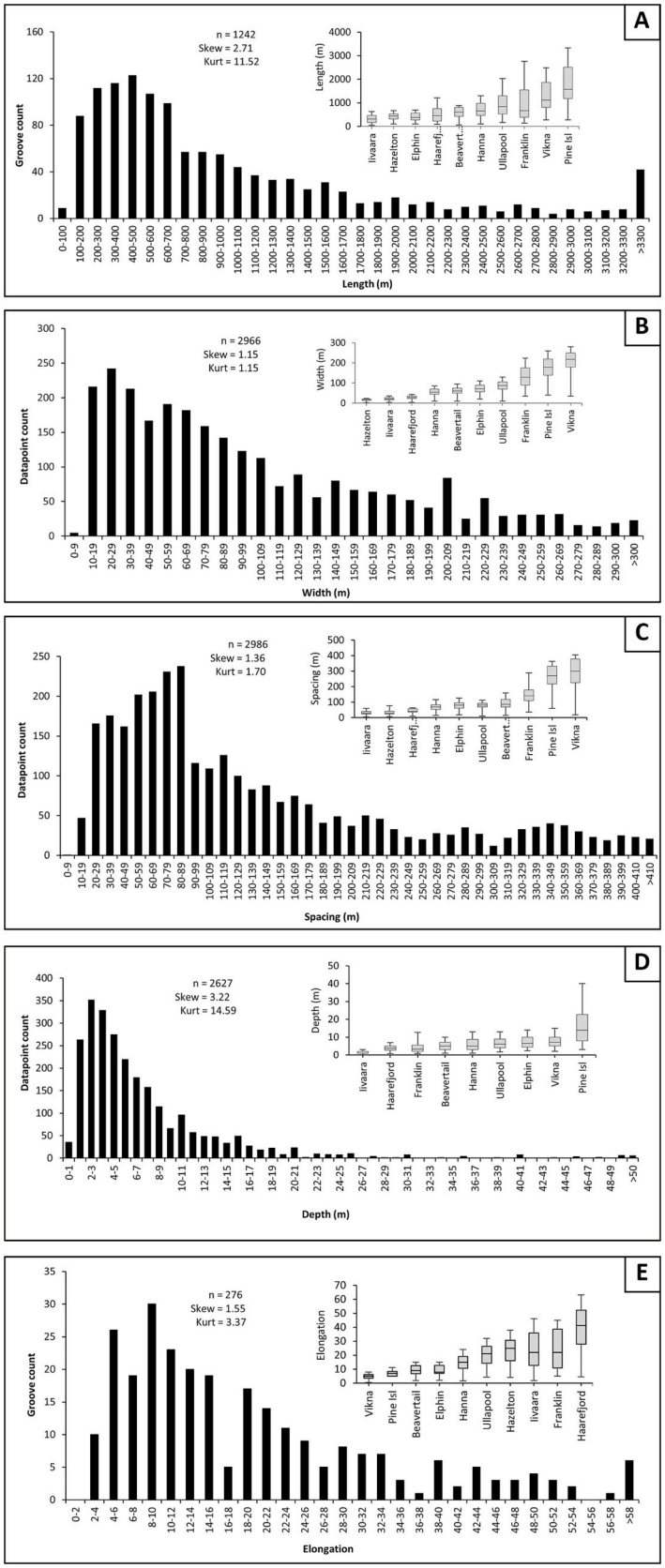

Fig. 17. Frequency distribution for the length (A), width (B), spacing (C), depth (D) and elongation (E) for the entire mapped population of BMGs. The statistical box plots for individual parameters show the 10th, 25th, 50th, 75th and 90th percentiles of the value range. Kurt = kurtosis.

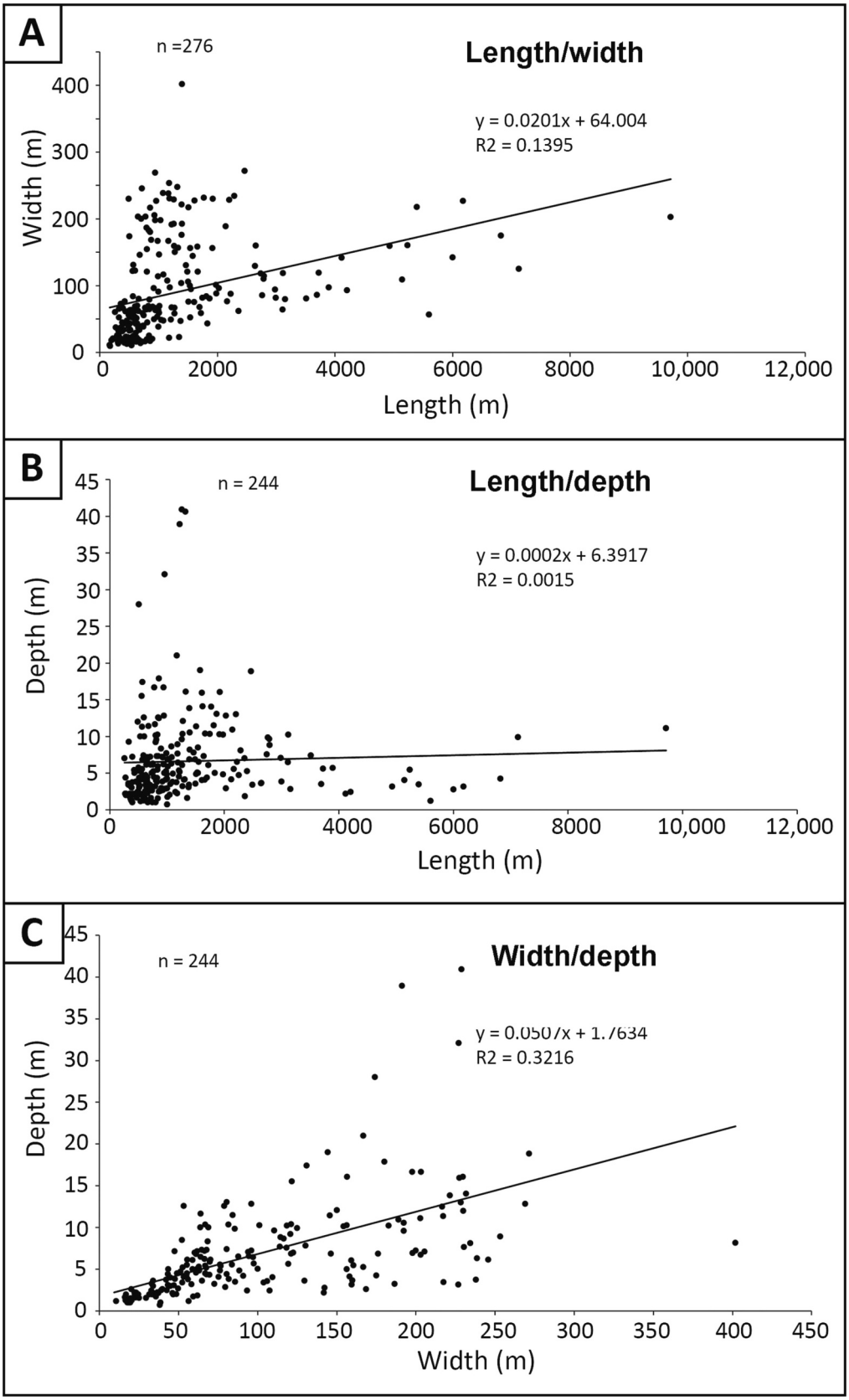

Fig. 18. Length, width and depth plotted against each other (A–C) for the entire sampled population. Each datapoint represents the mean value of that respective metric corresponding to a sampled groove. The plots are fitted with a linear trendline.

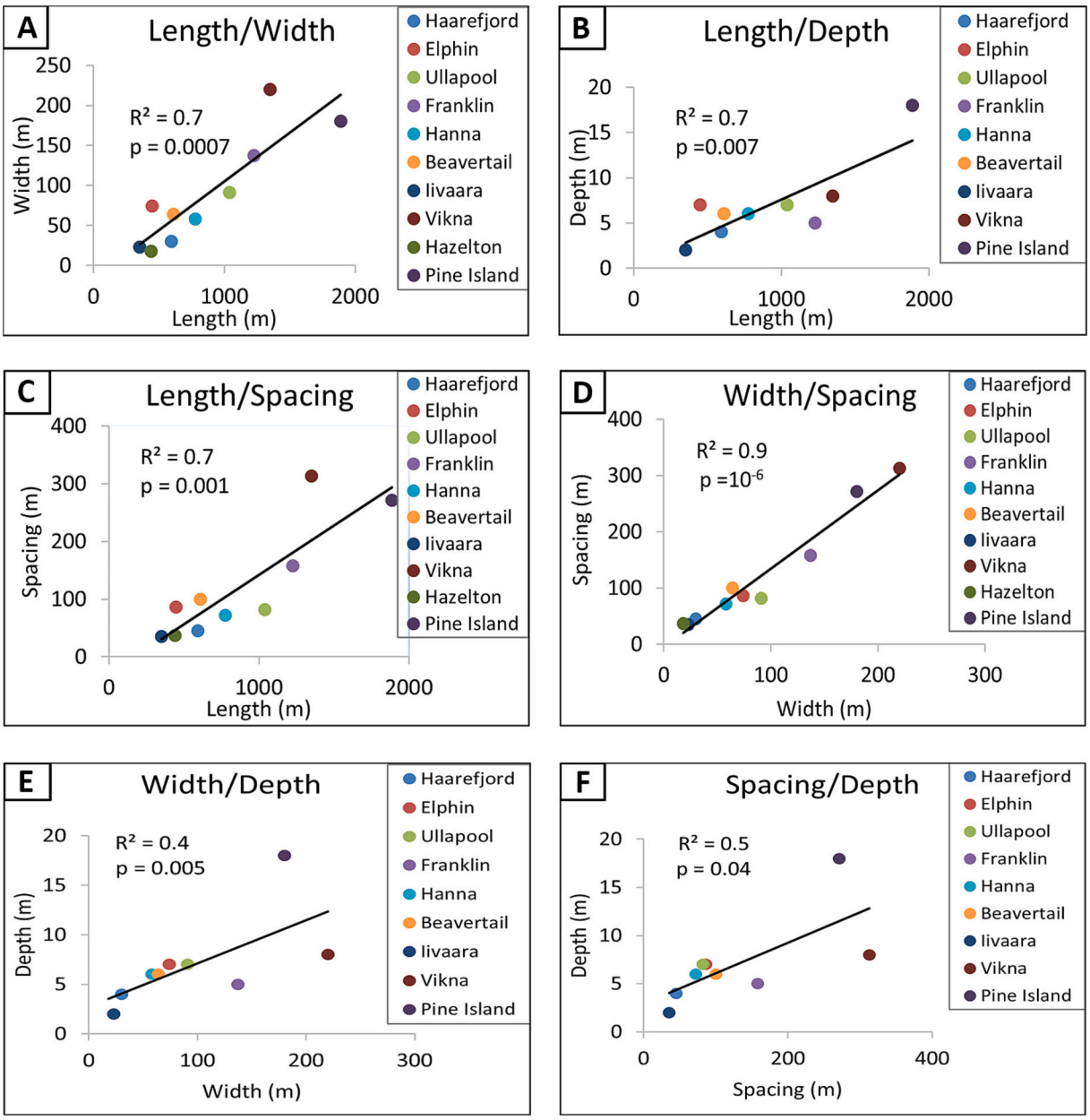

Fig. 19. Overall site-specific mean values for length, width, depth and spacing plotted against each other (A–F). Each value represents the overall mean of that metric for a study area (Table 2). The trendlines correspond to the linear equations. R^2 (written "R2" in the diagrams) indicates the correlation strength between plotted metrics, and the p-value represents the statistical significance. Note the low p-values on all graphs (<0.05; in Part D "10–6" means "10^{-6}"), suggesting that the correlations are statistically significant.

of plucking or abrasion would need to be validated by field evidence pertaining to BMGs at Hanna, Beavertail and Iivaara, so at this stage the results here should be regarded as provisional and only a starting point for further research.

Regarding the role of water erosion in BMG formation, which is notoriously difficult to quantify (Eyles, 2006) it is significant that the deepest BMGs reported both on-shore at Franklin (Smith, 1948; Hamilton and Ford, 2002; Table 2; Fig. 17D) and off-shore at Pine Island (Lowe and Anderson, 2003; Kirkham et al., 2019; Table 2; Fig. 17D) are associated with the effects of water erosion. At Franklin, the porous the Great Bear Formation limestone, has been affected by dissolution (Hamilton and Ford, 2002; see Section 3.4), contributing to BMG over deepening, alongside the formation of karstic landforms (Hamilton and Ford, 2002). The exceptional depth of the BMGs at Pine Island (Fig. 17D) could reasonably be associated with sudden discharges of large volumes of meltwater released following subglacial lake outbursts (Kirkham et al., 2019)., which would have resulted in highly erosive turbulent flow (Whipple et al., 2000). Overall, despite the limited and often equivocal data available, meltwater erosion could lead to BMGs attaining great depths through a pronounced channel erosion once a groove has been established (Newton et al., 2018).

In summary, morphometric correlations in conjunction with geological characteristics enable an initial assessment of the primary control factors over BMG development. Results so far seem to indicate that when fast-flowing ice is the primary controlling factor, the BMGs have the largest dimensions, lowest density and lowest elongation ratios, regardless of the bedrock geology. Where bedrock geology has been interpreted as the primary controlling factor, the BMG dimensions are comparable across lithologies, but they occupy the low end of the values spectrum and have formed under a range of glaciological conditions.

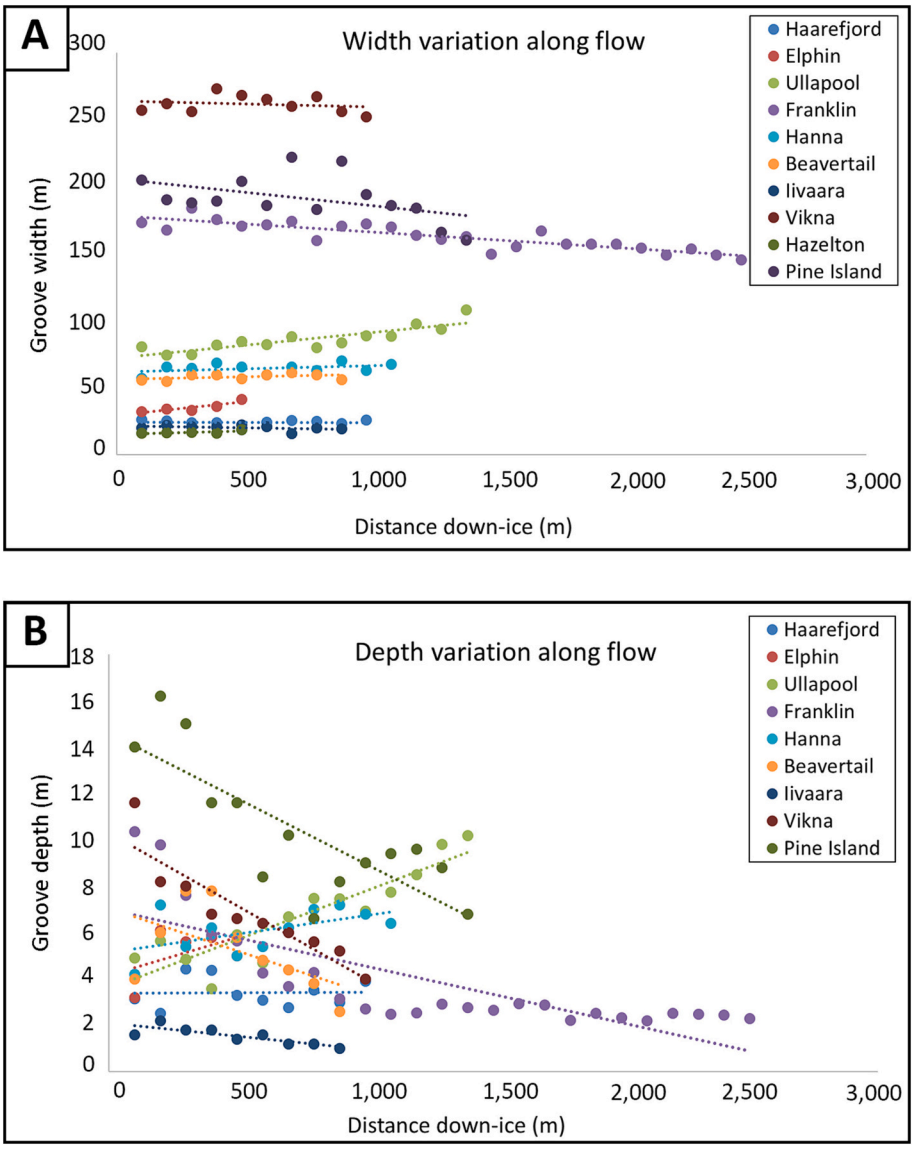

Fig. 20. Variation of width (A) and depth (B) along the grooves in the down-ice direction. Each datapoint represents the width and depth value, respectively, calculated as an average between five datapoints from five different grooves, whereby each datapoint is found at the same distance from the starting point of the groove. The starting point is at 100 m, so that the graphs are slightly offset from the x-axis, and the datapoints are spaced-out by 100 m, consistent with the protocol for sampling frequency (see Section 2.2). The ice-flow direction is from left to right.

5.4. Comparisons of BMGs and MSGLs

MSGLs are largely regarded as a diagnostic landform for identifying palaeo-ice streaming, commonly present in the middle-to-lower reaches of palaeo-ice stream landsystems (Clark, 1993; Stokes and Clark, 1999; Stokes and Clark, 2001; Ottesen et al., 2005), and their ongoing formation has been detected beneath fast-flowing ice in Antarctica (King et al., 2009). As for BMGs, it has been asserted that their formation is a direct result of enhanced glacial erosion in onset zones of fast-flow onset based on their common occurrence upstream from MSGLs (Bradwell et al., 2008; Eyles, 2012; Krabbendam et al., 2016; Eyles et al., 2018). Our results indicate that fast-flowing ice under streaming conditions could indeed be a primary control factor in BMG formation, capable of overriding geological controls, especially where BMGs are located within palaeo-ice stream landsystems which potentially relate to multiple phases of ice streaming (see Section 5.3). Here we attempt to establish whether BMGs and MSGLs represent a morphological continuum and to what extent BMGs and MSGLs reflect the same process-form relationship.

The morphometric data for MSGLs used for this comparison are extracted from the study of Spagnolo et al. (2014). The two landform datasets are of a similar magnitude, comprising nine sites for the MSGLs (Spagnolo et al., 2014) and ten sites for the BMGs from across the world. The MSGL population selected for width, spacing and amplitude measurements consists of 1929, 3543 and 1607 features, respectively (Spagnolo et al., 2014 and Table III therein), whereas for the BMGs these metrics were extracted from 276, 355 and 244 features, respectively (see Table 2). However, this discrepancy in numbers is balanced by the grid size on which measurements were undertaken, namely every 1000 m for MSGLs and every 100 m for mega-grooves, so the number of data points is within comparable ranges between the two landform types. For both BMGs and MSGLs the range for each metric is representative for 80 % of the landform population, comprising data between the 10th and the 90th percentile.

The protocols for measuring length and depth are identical in both studies (see Section 2.3). For MSGLs, width measurements were based on mapped polygons, approximated to highly elongate ellipses, and calculated as a function of the short axis of the ellipse (Spagnolo et al., 2014). For BMGs, width measurements were taken between points of inflexion in the slope angle, identified in cross-profiles. However, if these inflexion points were to be joined together, the result would be an elongate polygon delineating the BMG in planform, similar to basis on which MSGLs were mapped. Therefore, width measurements targeted the same feature in both landform types by using different graphic

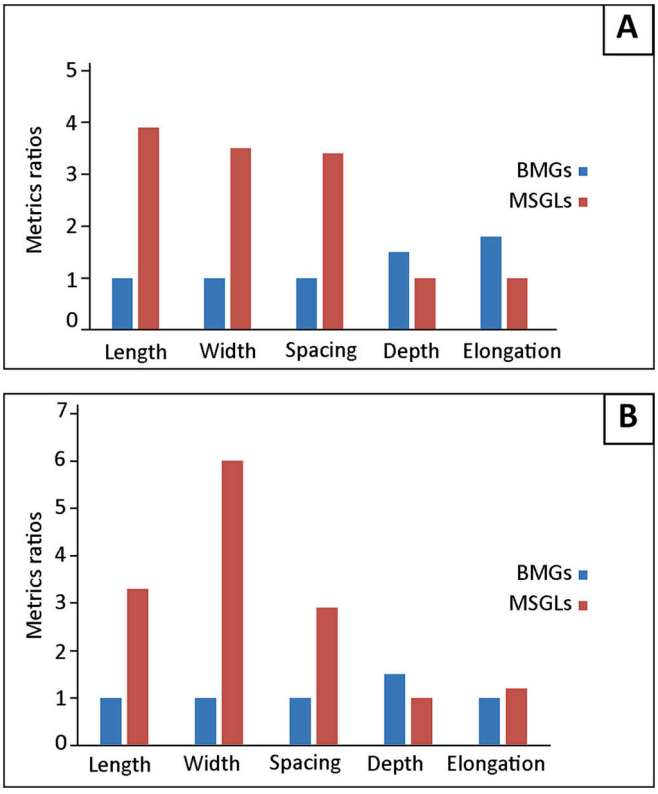

Fig. 21. Comparative representation of metrics for BMGs and MSGLs, based on mean values (A) and modal values (B) corresponding to the aggregated landform population for each landform type (see Table 4 for details). The metrics for the MSGLs were extracted from Spagnolo et al. (2014).

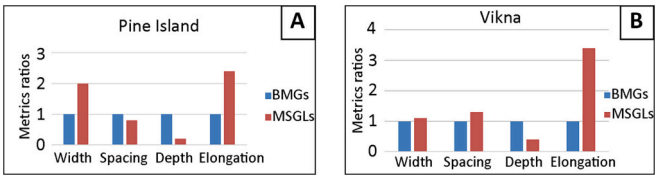

Fig. 22. Ratios of BMG and MSGL metrics from Pine Island (A) and Vikna (B), based on mean values listed in Table 5. The landform pairs belong to the same palaeo-ice stream landsystem for Pine Island, and to associated landsystems for Vikna. The MSGL metrics at Pine Island are extracted from Spagnolo et al. (2014), apart from width which is from Evans et al. (2006). At Vikna, in the absence of MSGL metrics from the associated Sklinnadjupet palaeo-ice stream landsystem, we used for comparison the MSGLs from three other landsystems along the Norwegian coast, where a similar transition from crystalline to sedimentary bedrock has been documented within each fast-flow onset zone, namely Skagerrak, Trænadjupet and Andfjorden (Ottesen et al., 2002 and 2005).

means. MSGL spacing was measured between adjacent landforms on *either* side, whereas for BMGs spacing values were extracted in relation to the next adjacent individual, moving in one direction across ice flow. Significant here is that in both cases spacing represents the distance between the centre line of landforms, and that both approaches carry out systematic measurements along and across ice flow, which likely return overall representative mean values for each site. Overall, despite differences in measuring protocols, the morphometric data of the two studies are regarded as broadly comparable.

The results (Table 4) show that BMGs are on average approximately 4 × shorter, 3.5 × narrower, 3.5 × more closely spaced and about 2 × deeper than MSGLs (Fig. 21A). Modal values for length, width and spacing are an order of magnitude higher for MSGLs. Significantly, there is no overlap between the ranges of modal values for any given metric, although the difference in depth is less pronounced. BMGs are therefore consistently shorter, narrower, deeper and denser than MSGLs (Fig. 21B), so at least morphometrically BMGs and MSGLs represent different landform populations.

BMGs and MSGLs are now analysed within the specific context of the palaeo-ice stream landsystem, in order to further refine landform comparisons and to explore potential morphogenetic links between the two landform types. The sites selected are Pine Island and Vikna because the BMGs there are situated in zones of fast-flow onset within ice-stream landsystems comprising MSGLs with available morphometric data. Although the glaciological conditions would have differed between the areas where the two landform types occur, due to ice velocity increasing down-flow, both BMGs and MSGLs can be regarded as having formed under fast-flow conditions, which produced BMGs with specific, large dimensions and small elongation ratios (see Section 5.3). The ratios of mean metrics between BMGs and their associated MSGLs were calculated (Table 5 and Fig. 22). The results show that BMGs are 1–1.6 × narrower, 0.8–1.5 × more closely spaced, and ~2.5 × shorter than their corresponding MSGLs (Fig. 22A and B). This shows that when analysed within a (palaeo)ice-stream landsystem, the discrepancy between dimensions of BMGs and their associated MSGLs is greatly reduced in comparison to results based on aggregated global populations.

High elongation ratios for MSGLs (mean 17:1, Spagnolo et al., 2014) is considered diagnostic of their formation through ice streaming (Stokes and Clark, 2002), whereas the opposite seems true for BMGs formed under the primary control of fast-ice flow conditions as the latter yield low mean values in the global population, with ratios of 5:1 and 7:1 (Table 2), which also renders them approximately 3 × less elongated than MSGLs. Potential underestimation of width due to the coarse resolution of the DEMs may have skewed the results towards higher values to some extent (see Section 2.4) and reduced elongation ratios, but the similarities of results remain striking considering all the other differences between the two sites (see Section 5.3). Despite both BMGs and MSGLs being elongate landforms formed subglacially, the discrepancy between their elongation ratios may reflect different geomorphic mechanisms. MSGLs evolve through an interplay between erosion and deposition, whereby the soft sediment in the deformation layer is transported and redeposited downstream (King et al., 2009), which can lead to MSGLs lengthening without widening, thus increasing elongation ratios over time. The low elongation ratios for the BMGs may reflect efficient lateral erosion leading to groove widening over time, which would yield low elongation ratios, assuming groove widening progresses at a higher rate than lengthening. These different feedback mechanisms driving landform development, underpinned by discrepancies in elongation ratios, show that BMGs and MSGLs are essentially different landform types, despite similarities in shape, but this does not rule out the likelihood of connections between them as component parts of ice-stream landsystems. One plausible link is that the supply of new debris eroded from BMGs upstream contributes to the deforming layer in MSGLs. BMGs also have the potential to act as "moulds" for the formation of ice keels that could plough through unlithified sediment downstream, contributing to MSGL formation (Clark et al., 2003; Piasecka et al., 2018).

In summary, quantitative comparisons between BMGs and MSGLs show that they represent two distinct landform types. Morphometrically they are discrete landform populations with BMGs approximately 4 × shorter, 3.5 × narrower, 3.5 × more closely spaced and about 2 × deeper than MSGLs. These differences are reduced by half when BMGs and MSGLs are analysed within their associated ice-stream landsystems. The most marked difference between BMGs and MSGLs resides in elongation ratios, explained through the likely different feedback mechanisms that drive their development and is interpreted here to strongly indicate that they represent different landform types.

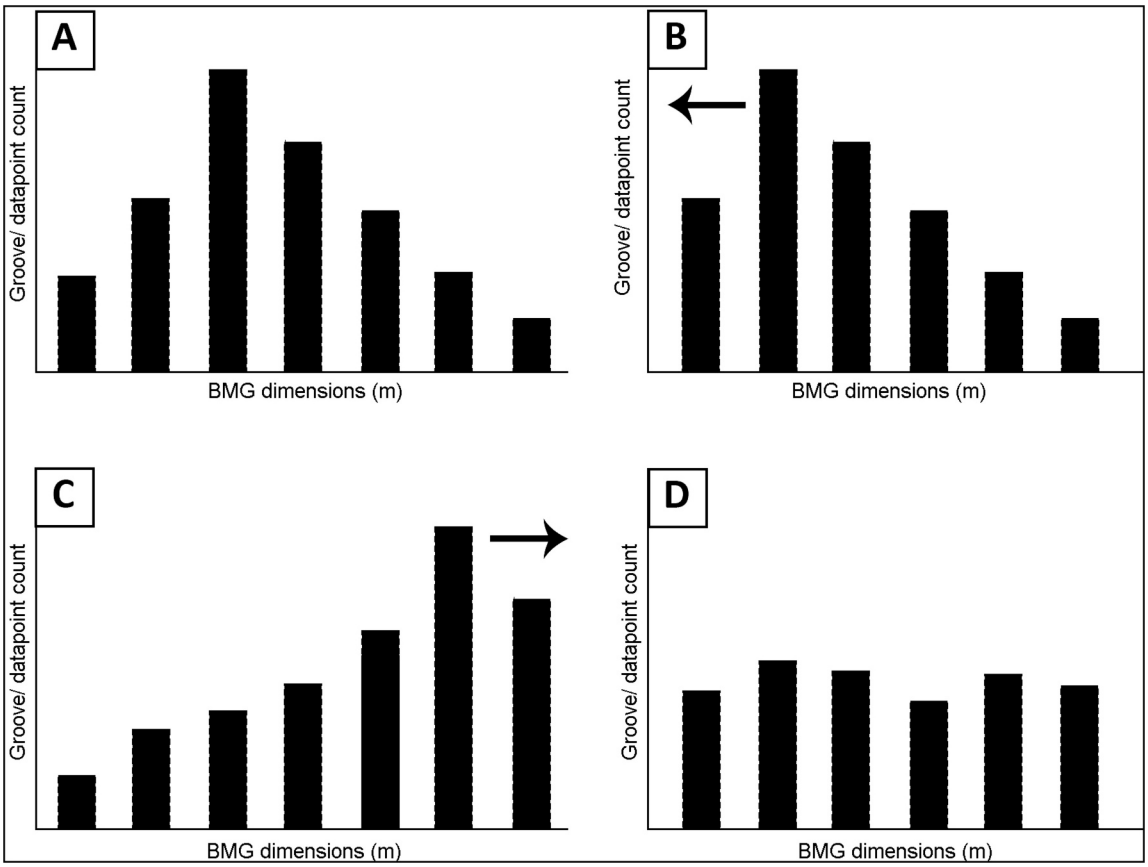

Fig. 23. Schematic diagram illustrating how BMG evolution over time would affect dimensional frequency distribution: A) the current distribution patterns for BMG length, width and depth are unimodal with a positive skew; B) mode shifting to the left, over time, would imply that the rate of new grooves being formed is higher than the rate at which grooves grow in size; C) mode shifting to the right, over time, would imply fewer new grooves being formed relative to the rate of development of existing grooves; D) a shift over time to a flat distribution with no obvious mode would imply an equilibrium between groove formation and development at all stages in their evolution.

Table 4
Summary of metrics for BMGs and MSGLs. The figures for MSGL metrics were extracted from Spagnolo et al. (2014). The range represent values between the 10th and the 90th per centile.

Landform	Length (m)			Width (m)			Spacing (m)			Depth (m)			Elongation ratios		
	Range	Mode	Mean	Range	Mode	Mean	Range	Mode	Mean	Range	Mode	Mean	Range	Mode	Mean
BMGs	224–2269	400–500	1018	21–210	20–30	98	35–315	80–90	134	2–15	3	7	5–41	8–10	20
MSGLs	940–9050	1000-2000	3967	90–720	100–200	348	140–960	200–300	458	1–9	1–2	4	6–33	6–8	17

5.5. How do BMGs evolve through time?

The result of quantitative analyses are used here to explore scenarios of BMG evolution through time, once the landforms have been initiated. Unlike drumlins (Ely et al., 2018), BMGs cannot shrink through erosion unless the intervening ridges are lowered at a higher rate than the grooves deepen, which would lead to landform obliteration. However, considering that any bedrock groove likely acts as a focus for erosion agents such as ice, debris and water (Boulton, 1974; Roberts et al., 2010), it could be argued that continued erosion leads to BMG growth through simultaneous lengthening, widening and deepening. Landform growth is suggested by the positive skew in the frequency distribution graphs for length, width and depth, reflected in the longer tail to the right of the mode (Fig. 17), and in the high values for kurtosis especially for length and depth, indicating that BMGs are capable of attaining large dimensions (c.f. Clark et al., 2009). BMG growth is also reflected in the positive correlations between length, width and depth at individual localities (see Section 4.2), despite such correlations being weak for the length/width and length/depth relationships (Fig. 18A and B). This means that, overall, the longer BMGs tend to be the deeper and wider specimens. The stronger and consistently positive width/depth correlations show that deep grooves are also wide (Section 4.2; Fig. 18C). This confirms that BMGs have a strong tendency to grow deeper as they become wider, a trend supported by the statistical significance of width/depth correlations (Table 3). This explains the high preservation potential of these landforms, as suggested by early studies (Smith, 1948; Funder, 1978). However, the steeper length/width trend than the length/depth trend, as shown by the comparison between equations corresponding to each linear trendline within individual sites (Figs. S7 and S8 in Supplementary Information 1), may indicate that lateral erosion is more efficient than vertical erosion. In theory, this would first result in adjacent grooves merging, leading to an increase in width and spacing (Fig. 19D), and eventually lead to landform obliteration unless the erosion cycle is somehow reset. This scenario could be best tested through future numerical modelling experiments.

Theoretically there are several scenarios of long-term BMG evolution

Table 5
The mean values for metrics BMG at Pine Island and Vikna, and for their associated MSGLs. The MSGL values at Pine Island are extracted from Spagnolo et al. (2014), apart from width which is from Evans et al. (2006). At Vikna, in the absence of MSGL metrics from the Sklinnadjupet palaeo-ice stream landsystem, we used for comparison the MSGLs from three other landsystems along the Norwegian coast, where a similar transition from crystalline to sedimentary bedrock has been documented within each fast-flow onset zone, namely Skagerrak, Trænadjupet and Andfjorden (Ottesen et al., 2002 and 2005). Where an interval was provided, the average value between the end members was calculated. The BMG metrics are mean values (Table 2). N/D = not determined.

Ice stream ID	Ice stream location	Landform and site ID	Mean length (m)	Length ratios (MSGLs/BMGs)	Mean width (m)	Width ratios (MSGLs/BMGs)	Mean Spacing (m)	Spacing ratios (MSGLs/BMGs)	Mean depth (m)	Depth ratios (BMGs/MSGLs)
Pine Island	West Antarctica	BMGs (Pine Island)	1580	2.5	180	1.6	270	0.8	14	4.6
		MSGLs (Pine Island)	4019		290		228		3	
Sklinnadjupet	W Norway	BMGs (Vikna)	1117	N/D	218	1–1.2	300	1.2-1.5	7	1.4–2
Norwegian Channel	SW Norway	MSGLs (Skagerrak)	N/D		275		400		3.5	
Trænadjupet	W Norway	MSGLs (Trænadjupet)	N/D		250		450		<5	
Tromsøflaket	N Norway	MSGLs (Andfjorden)	N/D		210		370		<3	

when considering the directions that the frequency distribution of landform metrics could evolve. They may remain unchanged, shift to the right/left of the current modal value, or become more evenly spread across the value range (Ely et al., 2018). Currently, the distribution patterns of the BMG metrics are unimodal, with a positive skew (Fig. 17A–D). For the distribution patterns to remain unchanged through time, the current equilibrium between the production rate of new, smaller grooves emerging in the system and the growth rate of the existing grooves needs to be maintained, so that the mode remains unchanged (Fig. 23A). The mode would shift to the left if the production rate of small grooves exceeded that of landform growth (Fig. 23B), and it would be expected to shift to the right if too few new grooves came into the system as the existing ones continued growing (Fig. 23C). Notably, at sites comprising the largest BMGs, the values of landform dimensions tend to be more widely and uniformly spread out across the range (Fig. 23D and Figs. S2–S5 in Supplementary Information 1). The same trend has been noted for drumlins, explained through landform initiation at different times during pattern evolution (Ely et al., 2018) and supported by results of statistical and numerical models (Fowler et al., 2013; Barchyn et al., 2016). Assuming the BMGs at Vikna and Pine Island are the most evolved landforms, the current distribution pattern may suggest a reduced preference for scaling relative to a mode as the BMGs mature (Fig. 23D). It is still not known whether this pattern emerges only under ice-streaming conditions, applicable so far to these two sites, or whether it is the end result of prolonged glacial erosion under slow flowing conditions given the necessary time for the landforms to grow (see Section 5.4). Modelling experiments will hopefully be able to test these scenarios in the future.

The distribution patterns lengths and widths are similar to those for drumlins, a possible explanation being that not enough time has yet passed for the landforms to attain larger dimensions (c.f. Clark et al., 2009). This explanation is difficult to test without knowing their age or how they were initiated, in addition to the fact that aggregated global populations may comprise landforms of different age. Knowing for how long a particular set of BMGs had been under the ice would enable comparison of samples that lay under ice sheets for a long time with those found in ice marginal areas and thereby enable calculation of BMG formation rates.

In summary, BMGs evolve by lengthening, widening and deepening, as suggested by the positive correlations between these metrics at all levels of analysis. The particularly strong positive correlation between width and depth may explain the high preservation potential of BMGs as they continue to deepen while becoming wider. As the BMGs attain larger dimensions, individual metrics show a reduced preference for scaling, reflected by the more evenly spread frequency distribution patterns. It is still uncertain whether this is the effect of fast-flowing ice or simply equifinality under any glaciological conditions.

Future research could advance understanding of BMG development through numerical modelling experiments. These could test rates of erosion in different bedrock substrates under varying glaciological conditions, which might also provide constraints on uncertain landform age from their dimensions. Empirical evidence remains key in validating geological controls over BMG formation and in assessing the efficiency of erosion mechanisms, where direct field observation remains essential. At the same time, analyses of morphometric data retrieved through remote sensing for BMGs and MSGLs within the same ice-stream landsystem could help elucidate links between the two types of landform and fast-ice flow (Table 5).

6. Conclusions

The results of landform measurements confirm that BMGs are elongate landforms of considerable length, depth and width in the suite of landforms formed subglacially, and with a high degree of parallelism to former regional ice-flow directions. Based on the aggregated global population, BMGs have lengths of 224–2269 m, widths of 21–210 m, depths of 2–15 m, elongation ratios of 5:1–41:1 and a spacing of 35–315 m. Morphometrically, the total sample of BMGs plot as a single landform population with a unimodal spatial distribution and overlapping value ranges for all metrics, which implies that they represent one landform type, similar to the case made previously for drumlins (Clark et al., 2009). There is a pronounced inter-site variability both in the spatial and the statistical distribution of the BMG metrics, as well as in the non-linear landform development of BMG length in relation to width and depth, likely due to highly variable local control factors, especially bedrock geology.

The BMGs associated with hypothesised or known sites of ice streaming are the largest in the dataset with mean lengths of over 1000 m and widths over 150 m, which is one order of magnitude longer and wider than BMGs at other sites, and have the lowest elongation ratios of 1:5–1:7, which is one order of magnitude lower than the rest of the dataset. This is interpreted as the result of enhanced lateral erosion induced by fast-flowing ice in contact with the bedrock, possibly over long periods of time. When bedrock geology is hypothesised to be the primary control, the BMGs have smaller dimensions, with plucking-dominated grooves occupying the mid-range position in the metrics spectrum, and abrasion-dominated grooves positioned at the lower end. There is independent evidence to suggest that the deepest BMGs may also have been enhanced by meltwater erosion. Strongly positive and consistent linear correlations between site-specific mean values for BMG

metrics, analysed across the site populations, show a uniformity in the development of BMG metrics. This points to an overarching scenario of BMG development likely to be inherent to the physics of the process of bedrock erosion by glacier ice.

Morphometrically BMGs and MSGLs plot as different populations. BMGs are on average approximately 4 × shorter, 3.5 × narrower, 3.5 × more closely spaced and about 2 × deeper. The lower elongation ratios of BMGs than MSGLs are the result of the different mechanisms of landform evolution, with the former widening through lateral erosion and the latter lengthening as soft sediment is mobilised and deposited downstream. Despite similarities in their morphology and occurrence within the same ice-stream landsystems, BMGs and MSGLs are different landform types due to their different morphometry and formation mechanisms.

Declaration of competing interest

The authors have no conflicts of interest to report.

Data availability

Data will be made available on request.

Acknowledgements

The authors are grateful to Neil Glasser and Stewart Jamieson for their suggestions which improved and clarified an early version of the manuscript. Thanks to Nikos Putkinen from the Geological Survey of Finland, for signposting the Iivaara site to us; to Brian Anderson, from Rice University of Texas, for making MN aware of GeoMapApp; to Terry Allen for providing the photograph of the Røde Ø Conglomerate. The Arctic DEM files were provided by the Polar Geospatial Centre under NSF-OPP awards 1043681, 1559691, and 1542736. Fieldwork in Scotland was supported by a QRA grant awarded to Mihaela Newton while a PhD student at Durham University, UK. The authors are grateful to the two anonymous reviewers who helped improve the clarity of this paper.

Appendix A. Supplementary data

Supplementary data to this article can be found online at https://doi.org/10.1016/j.geomorph.2023.108619.

References

Aitken, J.D., Cook, D.G., 1979. Geology, Sans Sault Rapids, District of Mackenzie; Geological Survey of Canada, "A" Series Map 1453A, 1 Sheet. https://doi.org/10.4095/123316 (Open Access).

Barchyn, T.E., Dowling, T.P., Stokes, C.R., Hugenholtz, C.H., 2016. Subglacial bed form morphology controlled by ice speed and sediment thickness. Geophys. Res. Lett. 43, 7572–7580. https://doi.org/10.1002/2016GL069558.

Batchelor, C.L., Margold, M., Krapp, M., Murton, D.K., Dalton, A.S., Gibbard, P.L., Stokes, C.R., Murton, J.B., Manica, A., 2019. The configuration of Northern Hemisphere ice sheets through the Quaternary. Nat. Commun. 10, 1–10. https://doi.org/10.1038/s41467-019-11601-2.

Boulton, G.S., 1974. Processes and patterns of glacial erosion. In: Coates, D.R. (Ed.), Glacial Geomorphology. University of New York, Binghampton, pp. 41–87.

Bradwell, T., 2005. Bedrock megagrooves in Assynt, NW Scotland. Geomorphology 65, 195–204. https://doi.org/10.1016/j.geomorph.2004.09.002.

Bradwell, T., Stoker, M., Larter, R., 2007. Geomorphological signature and flow dynamics of the Minch palaeo-ice stream, Northwest Scotland. J. Quat. Sci. 22, 609–617. https://doi.org/10.1002/jqs.1080.

Bradwell, T., Stoker, M., Krabbendam, M., 2008. Megagrooves and streamlined bedrock in NW Scotland: the role of ice streams in landscape evolution. Geomorphology 97, 135–156. https://doi.org/10.1016/j.geomorph.2007.02.040.

Bradwell, T., Small, D., Fabel, D., Smedley, R.K., Clark, C.D., Saher, M.H., Callard, S.L., Chiverrell, R.C., Dove, D., Moreton, S.G., Roberts, D.H., 2019. Ice-stream demise dynamically conditioned by trough shape and bed strength. Sci. Adv. 5, p.eaau1380 https://doi.org/10.1126/sciadv.aau1380.

British Geological Survey (BGS), 2008. Ullapool. Scotland Sheet 101E. Bedrock. 1:50,000 Geology Series.

Brown, V.H., 2012. Ice stream dynamics and pro-glacial lake evolution along the north-western margin of the Laurentide Ice Sheet. Unpublished PhD thesis. Durham University. http://etheses.dur.ac.uk/5917/.

Brown, V.H., Stokes, C.R., Ó Cofaigh, C., 2011. The glacial geomorphology of the north-west sector of the Laurentide Ice Sheet. J. Maps 7 (1), 409–428. https://doi.org/10.4113/jom.2011.1224.

Bugge, T., Knarud, R., Mørk, A., 1984. Bedrock geology on the mid-Norwegian continental shelf. In: Spencer, A.M. (Ed.), Petroleum Geology of the North European Margin. Springer, Dordrecht, pp. 271–283.

Bukhari, S., Eyles, N., Sookhan, S., Mulligan, R., Paulen, R., Krabbendam, M., Putkinen, N., 2021. Regional subglacial quarrying and abrasion below hard-bedded palaeo-ice streams crossing the Shield-Palaeozoic boundary of Central Canada: the importance of substrate control. Boreas 50, 781–805. https://doi.org/10.1111/bor.12522.

Chandler, B.M., Lovell, H., Boston, C.M., Lukas, S., Barr, I.D., Benediktsson, Í.Ö., Benn, D. I., Clark, C.D., Darvill, C.M., Evans, D.J.A., Ewertowski, M.W., 2018. Glacial geomorphological mapping: a review of approaches and frameworks for best practice. Earth Sci. Rev. 185, 806–846. https://doi.org/10.1016/j.earscirev.2018.07.015.

Clark, C.D., 1993. Mega-scale glacial lineations and cross-cutting ice-flow landforms. Earth Surf. Process. Landf. 18, 1–29. https://doi.org/10.1002/esp.3290180102.

Clark, C.D., Tulaczyk, S.M., Stokes, C.R., Canals, M., 2003. A groove-ploughing theory for the production of mega-scale glacial lineations, and implications for ice-stream mechanics. J. Glaciol. 49, 240–256. https://doi.org/10.3189/172756503781830719.

Clark, C.D., Hughes, A.L., Greenwood, S.L., Spagnolo, M., Ng, F.S., 2009. Size and shape characteristics of drumlins, derived from a large sample, and associated scaling laws. Quat. Sci. Rev. 28, 677–692. https://doi.org/10.1016/j.quascirev.2008.08.035.

Collinson, J.D., 1972. The Røde Ø Conglomerate of Inner Scoresby Sund and the Carboniferous and Permian Rocks West of the Schuchert Flod - A General Sedimentological Account. Meddelelser om Gronland 102. Reitzel, Copenhagen.

DigMapGB_50, 2016. Tile sc101e. Geological Map Data, British Geological Survey © UKRI 2016.

Dühnforth, M., Anderson, R.S., Ward, D., Stock, G.M., 2010. Bedrock fracture control of glacial erosion processes and rates. Geology 38, 423–426. https://doi.org/10.1130/G30576.1.

Duk-Rodkin, A., Hughes, O.L., 1993. Surficial Geology, Sans Sault Rapids, District of Mackenzie, Northwest Territories; Geological Survey of Canada, "A" Series Map 1784A, 1 Sheet. https://doi.org/10.4095/184008.

Duk-Rodkin, A., Barendregt, R.W., Froese, G.D., Weber, F., Enkin, R., Smith, I.R., Waters, P., Klassen, R., 2004. Timing and extent of Plio-Pleistocene glaciations in north-western Canada and east-central Alaska. In: Ehlers, J., Gibbard, P.L. (Eds.), Quaternary Glaciations e Extent and Chronology, Part II. Elsevier, Amsterdam, pp. 313–345. https://doi.org/10.1016/S1571-0866(04)80206-9.

Dunlop, P., Clark, C.D., 2006. The morphological characteristics of ribbed moraine. Quat. Sci. Rev. 25, 1668–1691. https://doi.org/10.1016/j.quascirev.2006.01.002.

Dunlop, P., Clark, C.D., Hindmarsh, R.C., 2008. Bed ribbing instability explanation: testing a numerical model of ribbed moraine formation arising from coupled flow of ice and subglacial sediment. J. Geophys. Res. Earth Surf. 113 (F3) https://doi.org/10.1029/2007JF000954.

Ely, J.C., Clark, C.D., Spagnolo, M., Stokes, C.R., Greenwood, S.L., Hughes, A.L., Dunlop, P., Hess, D., 2016. Do subglacial bedforms comprise a size and shape continuum? Geomorphology 257, 108–119. https://doi.org/10.1016/j.geomorph.2016.01.001.

Ely, J.C., Clark, C.D., Spagnolo, M., Hughes, A.L., Stokes, C.R., 2018. Using the size and position of drumlins to understand how they grow, interact and evolve. Earth Surf. Process. Landf. 43, 1073–1087. https://doi.org/10.1002/esp.4241.

Evans, J., Dowdeswell, J.A., Ó Cofaigh, C., Benham, T.J., Anderson, J.B., 2006. Extent and dynamics of the West Antarctic Ice Sheet on the outer continental shelf of Pine Island Bay during the last glaciation. Mar. Geol. 230, 53–72. https://doi.org/10.1016/j.margeo.2006.04.001.

Evans, D.J.A., Newton, M., Roberts, D.H., Stokes, C.R., 2023. Characteristics and formation of bedrock mega-grooves (BMGs) in glaciated terrain: 2 – conceptual models of BMG origin. Geomorphology 427, 1–18. https://doi.org/10.1016/j.geomorph.2023.108620.

Evans, D.J.A., Phillips, E.R., Atkinson, N., 2021a. Glacitectonic rafts and their role in the generation of Quaternary subglacial bedforms and deposits. Quat. Res. 104, 104–135. https://doi.org/10.1017/qua.2021.11.

Evans, D.J.A., Smith, I.R., Gosse, J., Galloway, J.M., 2021b. Glacial landforms and sediments (landsystem) of the smoking Hills area, Northwest Territories, Canada: implications for regional Pliocene-Pleistocene Laurentide Ice Sheet dynamics. Quat. Sci. Rev. 262, 106958 https://doi.org/10.1016/j.quascirev.2021.106958.

Evenchick, C.A., McMechan, M.E., Mustard, Ferri, F., Waldron, J.W.F., 2008. Geology, Hazelton, British Columbia. Geological Survey of Canada, Open File 5704. BC Ministry of Energy, Mines and Petroleum Resources, Petroleum Geology Open Files 2008-6, Scale 1: 125 000.

Eyles, N., 2006. The role of meltwater in glacial processes. Sediment. Geol. 190, 257–268. https://doi.org/10.1016/j.sedgeo.2006.05.018.

Eyles, N., 2012. Rock drumlins and megaflutes of the Niagara Escarpment, Ontario, Canada: a hard bed landform assemblage cut by the Saginaw-Huron Ice Stream. Quat. Sci. Rev. 55, 34–49. https://doi.org/10.1016/j.quascirev.2012.09.001.

Eyles, N., Putkinen, N., 2014. Glacially-megalineated limestone terrain of Anticosti Island, Gulf of St. Lawrence, Canada; onset zone of the Laurentian Channel ice stream. Quat. Sci. Rev. 88, 125–134. https://doi.org/10.1016/j.quascirev.2014.01.015.

Eyles, N., Putkinen, N., Sookhan, S., Arbelaez-Moreno, L., 2016. Erosional origin of drumlins and megaridges. Sediment. Geol. 338, 2–23. https://doi.org/10.1016/j.sedgeo.2016.01.006.
Eyles, N., Moreno, L.A., Sookhan, S., 2018. Ice streams of the late Wisconsin Cordilleran Ice Sheet in western North America. Quat. Sci. Rev. 179, 87–122. https://doi.org/10.1016/j.quascirev.2017.10.027.
Fallas, K.M., 2013. Geology, Mahony Lake (Southeast), Northwest Territories; Geological Survey of Canada, Canadian Geoscience Map 90, Scale 1:100 000. https://doi.org/10.4095/292282.
Fettes, D.J., Long, C.B., Bevins, R.E., Max, M.D., Oliver, G.J.H., Primmer, T.J., Thomas, L. J., Yardley, B.W.D., 1985. Grade and time of metamorphism in the Caledonide Orogen of Britain and Ireland. Geol. Soc. Lond. Mem. 9, 41–53. https://doi.org/10.1144/GSL.MEM.1985.009.01.03.
Fossen, H., 2016. Structural Geology. Cambridge University Press, Cambridge.
Fowler, A.C., Spagnolo, M., Clark, C.D., Stokes, C.R., Hughes, A.L.C., Dunlop, P., 2013. On the size and shape of drumlins. Geomathematics 4, 155–165. https://doi.org/10.1007/s13137-013-0050-0.
Funder, S., 1978. Glacial flutings in bedrock, an observation in East Greenland. Bull. Geol. Soc. Den. 27, 9–13.
Geological Survey of Finland, 2016. Bedrock of Finland 1:200,000. https://hakku.gtk.fi/en/.
Graham, A.G., Larter, R.D., Gohl, K., Dowdeswell, J.A., Hillenbrand, C.D., Smith, J.A., Evans, J., Kuhn, G., Deen, T., 2010. Flow and retreat of the late Quaternary Pine Island-Thwaites palaeo-ice stream, West Antarctica. J. Geophys. Res. Earth Surf. 115 (F3) https://doi.org/10.1029/2009JF001482.
Gravenor, C.P., Meneley, W.A., 1958. Glacial flutings in central and northern Alberta. Am. J. Sci. 256, 715–728. https://doi.org/10.2475/ajs.256.10.715.
Hamilton, J., Ford, D., 2002. Karst geomorphology and hydrogeology of the Bear Rock Formation—a remarkable dolostone and gypsum megabreccia in the continuous permafrost zone of Northwest Territories, Canada. Carbonates Evaporites 17, 114–115.
Heikkinen, O., Tikkanen, M., 1989. Drumlins and flutings in Finland: their relationships to ice movement and to each other. Sediment. Geol. 62, 349–355. https://doi.org/10.1016/0037-0738(89)90124-3.
Henriksen, N., 1983. Geological Map of RØdefjord 70 Ø3 Nord 1: 100,000. Map Compiled by Henriksen in 1977. Geological Survey of Greenland.
Hillier, J.K., Smith, M.J., Clark, C.D., Stokes, C.R., Spagnolo, M., 2013. Subglacial bedforms reveal an exponential size–frequency distribution. Geomorphology 190, 82–91. https://doi.org/10.1016/j.geomorph.2013.02.017.
Hillier, J.K., Kougioumtzoglou, I.A., Stokes, C.R., Smith, M.J., Clark, C.D., Spagnolo, M. S., 2016. Exploring explanations of subglacial bedform sizes using statistical models. PloS One 11, e0159489. https://doi.org/10.1371/journal.pone.0159489.
Hume, G.S., 1954. In: The Lower Mackenzie River area, Northwest Territories and Yukon: Geological Survey of Canada Memoir, p. 273. https://doi.org/10.4095/101498.
Iverson, N.R., 1991. Morphology of glacial striae: implications for abrasion of glacier beds and fault surfaces. Bull. Geol. Soc. Am. 103, 1308–1316. https://doi.org/10.1130/0016-7606(1991)103%3C1308:MOGSIF%3E2.3.CO;2.
Jezek, K., Wu, X., Gogineni, P., Rodríguez, E., Freeman, A., Rodriguez-Morales, F., Clark, C.D., 2011. Radar images of the bed of the Greenland Ice Sheet. Geophys. Res. Lett. 38, L01501 https://doi.org/10.1029/2010GL045519.
King, E.C., Hindmarsh, R.C., Stokes, C.R., 2009. Formation of mega-scale glacial lineations observed beneath a West Antarctic ice stream. Nat. Geosci. 2, 585–588. https://doi.org/10.1038/ngeo581.
Kirkham, J.D., Hogan, K.A., Larter, R.D., Arnold, N.S., Nitsche, F.O., Golledge, N.R., Dowdeswell, J.A., 2019. Past water flow beneath Pine Island and Thwaites glaciers, West Antarctica. Cryosphere 13, 1959–1981. https://doi.org/10.5194/tc-13-1959-2019.
Krabbendam, M., Bradwell, T., 2011. Lateral plucking as a mechanism for elongate erosional glacial bedforms: explaining megagrooves in Britain and Canada. Earth Surf. Process. Landf. 36, 1335–1349. https://doi.org/10.1002/esp.2157.
Krabbendam, M., Bradwell, T., 2014. Quaternary evolution of glaciated gneiss terrains: pre-glacial weathering vs. Glacial erosion. Quat. Sci. Rev. 95, 20–42. https://doi.org/10.1016/j.quascirev.2014.03.013.
Krabbendam, M., Glasser, N.F., 2011. Glacial erosion and bedrock properties in NW Scotland: abrasion and plucking, hardness and joint spacing. Geomorphology 130, 374–383. https://doi.org/10.1016/j.geomorph.2011.04.022.
Krabbendam, M., Prave, T., Cheer, D., 2008. A fluvial origin for the Neoproterozoic Morar Group, NW Scotland; implications for Torridon-Morar group correlation and the Grenville Orogen Foreland Basin. J. Geol. Soc. 165, 379–394. https://doi.org/10.1144/0016-76492007-076.
Krabbendam, M., Eyles, N., Putkinen, N., Bradwell, T., Arbelaez-Moreno, L., 2016. Streamlined hard beds formed by palaeo-ice streams: a review. Sediment. Geol. 338, 24–50. https://doi.org/10.1016/j.sedgeo.2015.12.007.
Lawson, T.J., 1996. Glacial striae and former ice movement: the evidence from Assynt, Sutherland. Scott. J. Geol. 32, 59–65. https://doi.org/10.1144/sjg32010059.
Lehijärvi, M., 1960. The Alkaline District of Iivaara, Kuusamo, Finland. Bull. Comm. Géol. Fin. 185.
Lehtinen, M., Nurmi, P.A., Ramo, O.T., 2005. Precambrian Geology of Finland. Elsevier, Amsterdam.
Linton, D.L., 1963. The forms of glacial erosion. Trans. Inst. Br. Geogr. 33, 1–28.
Livingstone, S.J., Storrar, R.D., Hillier, J.K., Stokes, C.R., Clark, C.D., Tarasov, L., 2015. An ice-sheet scale comparison of eskers with modelled subglacial drainage routes. Geomorphology 246, 104–112. https://doi.org/10.1016/j.geomorph.2015.06.016.
Lowe, A.L., Anderson, J.B., 2002. Reconstruction of the West Antarctic ice sheet in Pine Island Bay during the last Glacial Maximum and its subsequent retreat history. Quat. Sci. Rev. 21, 1879–1897. https://doi.org/10.1016/S0277-3791(02)00006-9.
Lowe, A.L., Anderson, J.B., 2003. Evidence for abundant subglacial meltwater beneath the paleo-ice sheet in Pine Island Bay, Antarctica. J. Glaciol. 49, 125–138. https://doi.org/10.3189/172756503781830971.
Margold, M., Stokes, C.R., Clark, C.D., 2015. Ice streams in the Laurentide Ice Sheet: identification, characteristics and comparison to modern ice sheets. Earth Sci. Rev. 143, 117–146. https://doi.org/10.1016/j.earscirev.2015.01.011.
McLaren, D.J., 1962. Middle and early Devonian Rhynchonelloid Brachiopods from Western Canada. Bull. Geol. Surv. Can. 86 https://doi.org/10.4095/100604.
Newton, M., 2022. The origin of bedrock mega-grooves in glaciated terrain. Unpublished PhD thesis. Durham University. http://etheses.dur.ac.uk/14349/.
Newton, M., Evans, D.J.A., Roberts, D.H., Stokes, C.R., 2018. Bedrock mega-grooves in glaciated terrain: a review. Earth Sci. Rev. 185, 57–79. https://doi.org/10.1016/j.earscirev.2018.03.007.
Nitsche, F.O., Gohl, K., Larter, R.D., Hillenbrand, C.D., Kuhn, G., Smith, J.A., Jacobs, S.S., Anderson, J.B., Jakobsson, M., 2013. Paleo ice flow and subglacial meltwater dynamics in Pine Island Bay, West Antarctica. Cryosphere 7, 249–262. https://doi.org/10.5194/tc-7-249-2013.
Ottesen, D., Dowdeswell, J.A., Rise, L., Rokoengen, K., Henriksen, S., 2002. Large-scale morphological evidence for past ice-stream flow on the mid-Norwegian continental margin. Geol. Soc. Lond. Spec. Publ. 203, 245–258. https://doi.org/10.1144/GSL.SP.2002.203.01.13.
Ottesen, D., Dowdeswell, J.A., Rise, L., 2005. Submarine landforms and the reconstruction of fast-flowing ice streams within a large Quaternary ice sheet: the 2500-km-long Norwegian-Svalbard margin (57–80 N). Geol. Soc. Am. Bull. 117, 1033–1050. https://doi.org/10.1130/B25577.1.
Peach, B.N., Horne, J., Gunn, W., Clough, C.T., Teall, J.J.H., Hinxman, L.W., 1907. The Geological Structure of the North-West Highlands of Scotland. HM Stationery Office, London.
Piasecka, E.D., Stokes, C.R., Winsborrow, M.C., Andreassen, K., 2018. Relationship between mega-scale glacial lineations and iceberg ploughmarks on the Bjørnøyrenna Palaeo-Ice Stream bed, Barents Sea. Mar. Geol. 402, 153–164. https://doi.org/10.1016/j.margeo.2018.02.008.
Punkari, M., 1980. The ice lobes of the scandinavian ice sheet during the deglaciation in Finland. Boreas 9, 307–310. https://doi.org/10.1111/j.1502-3885.1980.tb00710.x.
Roberts, D.H., Long, A.J., 2005. Streamlined bedrock terrain and fast ice flow, Jakobshavns Isbrae, West Greenland: implications for ice stream and ice sheet dynamics. Boreas 34, 25–42. https://doi.org/10.1111/j.1502-3885.2005.tb01002.x.
Roberts, D.H., Long, A.J., Davies, B.J., Simpson, M.J., Schnabel, C., 2010. Ice stream influence on West Greenland ice sheet dynamics during the last Glacial Maximum. J. Quat. Sci. 25, 850–864. https://doi.org/10.1002/jqs.1354.
Roberts, D.H., Rea, B.R., Lane, T.P., Schnabel, C., Rodés, A., 2013. New constraints on Greenland ice sheet dynamics during the last glacial cycle: evidence from the Uummannaq ice stream system. J. Geophys. Res. Earth Surf. 118, 519–541. https://doi.org/10.1002/jgrf.20032.
Sharpe, D.R., Shaw, J., 1989. Erosion of bedrock by subglacial meltwater, Cantley, Quebec. Bull. Geol. Soc. Am. 101, 1011–1020. https://doi.org/10.1130/0016-7606(1989)101%3C1011:EOBBSM%3E2.3.CO;2.
Shaw, J., 2002. The meltwater hypothesis for subglacial bedforms. Quat. Int. 90, 5–22. https://doi.org/10.1016/S1040-6182(01)00089-1.
Sindern, S., Kramm, U., 2000. Volume characteristics and element transfer of fenite aureoles: a case study from the Iivaara alkaline complex, Finland. Lithos 51, 75–93. https://doi.org/10.1016/S0024-4937(99)00075-4.
Smith, H.T.U., 1948. Giant glacial grooves in Northwest Canada. Am. J. Sci. 246, 503–514. https://doi.org/10.2475/ajs.246.8.503.
Smith, M.J., Clark, C.D., 2005. Methods for the visualization of digital elevation models for landform mapping. Earth Surf. Process. Landf. 30, 885–900. https://doi.org/10.1002/esp.1210.
Smith, A.M., Bentley, C.R., Bingham, R.G., Jordan, T.A., 2012. Rapid subglacial erosion beneath Pine Island glacier, West Antarctica. Geophys. Res. Lett. 39, L12501 https://doi.org/10.1029/2012GL051651.
Sørensen, K., 1970. Geological map of the northern Røde Fjord area 1:50, 000. Field observations. In: Geological Survey of Denmark and Greenland.
Spagnolo, M., Clark, C.D., Ely, J.C., Stokes, C.R., Anderson, J.B., Andreassen, K., Graham, A.G., King, E.C., 2014. Size, shape and spatial arrangement of mega-scale glacial lineations from a large and diverse dataset. Earth Surf. Process. Landf. 39, 1432–1448. https://doi.org/10.1002/esp.3532.
Stemmerik, L., Piasecki, S., 2004. Isotopic evidence for the age of the Røde Ø Conglomerate, inner Scoresby Sund, East Greenland. Bull. Geol. Soc. Den. 51, 137–140.
Stoker, M.S., 1995. The influence of glacigenic sedimentation on slope-apron development on the continental margin off Northwest Britain. Geol. Soc. Lond. Spec. Publ. 90, 159–177. https://doi.org/10.1144/GSL.SP.1995.090.01.10.
Stoker, M., Bradwell, T., 2005. The Minch palaeo-ice stream, NW sector of the British-Irish Ice Sheet. J. Geol. Soc. 162, 425–428. https://doi.org/10.1144/0016-764904-151.
Stoker, M.S., Holmes, R., 1991. Submarine end-moraines as indicators of Pleistocene ice-limits off Northwest Britain. J. Geol. Soc. 148, 431–434. https://doi.org/10.1144/gsjgs.148.3.0431.
Stokes, C.R., Clark, C.D., 1999. Geomorphological criteria for identifying Pleistocene ice streams. Ann. Glaciol. 28, 67–74. https://doi.org/10.3189/172756499781821625.
Stokes, C.R., Clark, C.D., 2001. Palaeo-ice streams. Quat. Sci. Rev. 20, 1437–1457. https://doi.org/10.1016/S0277-3791(01)00003-8.

Stokes, C.R., Clark, C.D., 2002. Are long subglacial bedforms indicative of fast ice flow? Boreas 31, 239–249. https://doi.org/10.1111/j.1502-3885.2002.tb01070.x.
Stokes, C.R., Spagnolo, M., Clark, C.D., Ó Cofaigh, C., Lian, O.B., Dunstone, R.B., 2013. Formation of mega-scale glacial lineations on the Dubawnt Lake Ice Stream bed: 1. size, shape and spacing from a large remote sensing dataset. Quat. Sci. Rev. 77, 190–209. https://doi.org/10.1016/j.quascirev.2013.06.003.
Storrar, R.D., Stokes, C.R., Evans, D.J.A., 2014. Morphometry and pattern of a large sample (> 20,000) of Canadian eskers and implications for subglacial drainage beneath ice sheets. Quat. Sci. Rev. 105, 1–25. https://doi.org/10.1016/j.quascirev.2014.09.013.
Sugden, D.E., 1974. In: Landscapes of glacial erosion in Greenland and their relationship to ice, topographic and bedrock conditions.. Institute of British Geographers Special Publication 7, pp. 177–195.
Sutinen, R., Hyvönen, E., Närhi, P., Haavikko, P., Piekkari, M., Middleton, M., 2010. Sedimentary anisotropy diverges from flute trends in south-east finnish Lapland. Sediment. Geol. 232, 190–197. https://doi.org/10.1016/j.sedgeo.2010.02.008.
Tassonyi, E.J., 1969. Subsurface geology, lower Mackenzie River and Anderson River area, District of Mackenzie. Geol. Surv. Can. Pap. 68-25.
Whipple, K.X., Hancock, G.S., Anderson, R.S., 2000. River incision into bedrock: mechanics and relative efficacy of plucking, abrasion, and cavitation. Bull. Geol. Soc. Am. 112, 490–503. https://doi.org/10.1130/0016-7606(2000)112%3C490:RIIBMA%3E2.0.CO;2.
Witkind, I.J., 1978. Giant glacial grooves at the north end of Mission Range, Northwest Montana. J. Res. US Geol. Surv. 6, 425–433.
Zumberge, J.H., 1955. Glacial erosion in tilted rock layers. J. Geol. 63, 149–158. https://doi.org/10.1086/626241.